Grid planning by using a synthetic grid model

With the integration of EVs

Master's thesis in Sustainable power engineering and electromobility

Anton Corneliusson

DEPARTMENT EARTH, SPACE AND ENVIRONMENT

CHALMERS UNIVERSITY OF TECHNOLOGY
Gothenburg, Sweden 2025
www.chalmers.se

MASTER's THESIS 2025

Grid planning by using a synthetic grid model

With the integration of EVs

Anton Corneliusson

CHALMERS
UNIVERSITY OF TECHNOLOGY

Department of Space, Earth and Environment
Division of Energy Technology
Chalmers University of Technology
Gothenburg, Sweden 2025

Grid planning by using a synthetic grid model
With the integration of EVs
Anton Corneliusson

Supervisor: Therese Lundblad, Department of Space, Earth and Environment
Supervisor: Josefine Grundius, Ellevio
Examiner: Maria Taljegård, Department of Space, Earth and Environment

Master Thesis 2025
Department of Space, Earth and Environment
Division of Energy Technology
Chalmers University of Technology
SE-412 96 Gothenburg
Sweden
Telephone +46 31 772 1000

Typeset in LaTeX
Printed by Chalmers Reproservice
Gothenburg, Sweden 2025

Grid planning by using a synthetic grid model
With the integration of EVs
Anton Corneliusson
Department of Earth, Space and Environment
Chalmers University of Technology

Abstract

The increasing integration of electric vehicles (EVs) presents new challenges for low voltage (LV) local and distribution grids. This thesis evaluates the impact of widespread residential EV charging by comparing real grid data from the Swedish distribution system operator (DSO) Ellevio with estimates from the synthetic Reference Electricity Grid Analysis (REGAL) model. Focusing on three residential-dominated areas under a scenario of 100% EV penetration, the study assesses peak load increases and substation utilization using measured grid data and real EV charging profiles. The model's accuracy is evaluated through parameter comparisons. Results indicate that peak loads may increase by up to 40%, with REGAL generally overestimating demand. While the model proves useful for early-stage planning in predominantly residential areas, its applicability diminishes in areas with significant commercial loads. The study highlights the importance of aligning synthetic models with local conditions as EV adoption accelerates.

Keywords: EVs, LV grids, REGAL, Grid planning, Load forecasting, Residential charging, Load Analysis

Acknowledgements

I would like to express my gratitude to my two supervisors, Therese Lundbald from Chalmers and Josefine Grundius from Ellevio. Therese provided excellent feedback and valuable suggestions throughout the thesis, especially regarding alternative data analysis. Josefine offered continuous support with the use of various software tools and contributed many insightful ideas. I am also grateful for the opportunity she provided to engage in discussions with professionals at Ellevio, which deepened my understanding of the real-world challenges facing the electricity grid.

I would also like to thank Maria Taljegård, who played an essential role in making this thesis possible.

Lastly, I want to thank my family and friends for their encouragement, which helped me stay motivated throughout this journey.

Anton Corneliusson, Gothenburg, June 2025

List of Acronyms

Below is the list of acronyms that have been used throughout this thesis listed in alphabetical order:

AC	Alternating Current
BEV	Battery Electric Vehicle
DC	Direct Current
DER	Distributed Energy Resources
DSO	Distribution System Operator
Ei	Energimarknadsinspektionen
EU	European Union
EV	Electric Vehicle
HC	Hosting Capacity
IBR	Inverter Based resources
LV	Low Voltage
MAPE	Mean Average Percentage Error
MV	Medium voltage
PHEV	Plug-in Hybrid Electric Vehicle
PV	Photo Voltaic
REGAL	Reference Electricity Grid Analysis
SCC	Short-circuit capacity
SOC	State of Charge
Svk	Svenska Kraftnät
THD	Total Harmonic Distortion
V2G	Vehicle-to-grid

Nomenclature

Below is the nomenclature of indices, sets, Source or Models, parameters, and variables that have been used throughout this thesis.

Indices

c	Index for EV charging profile
h	Index for the harmonic order
i	Index for customer number
j	Index for substation number
m	Index for cell number
n	Index for iteration number
t	Index for time step

Sets

C_j	Set of selected EV profiles at substation j
com	Set of commercial customers
res	Set of residential customers
tot	Set of all/total customers

Source or Models

Ellevio	Refers to real measured data from the DSO
REGAL	Refers to the estimated data from the synthetic grid model

Parameters

a, b, c	Denotes the three phases
E	Active energy consumption measured in kWh
J	Number of substations
M	Number of cells
N	Number of iterations or amount of a quantity
P	Active power consumption measured in kWh/h
S	Substation capacity measured in kVA
U	Denotes the voltage, measured in V
Δ	Denotes the percentage change
μ	Denotes the mean value or share
σ	Denotes the standard deviation
$MAPE$	Denotes the deviation measured in %
THD	Denotes the total harmonic distortion [-]

Variables

$E_{res,year,j}$	Annual active energy consumption at substation j
$k_{1/2}$	Velander constant 1 or 2
$k_{1/2,n}^{Est}$	Estimated Velander constant at iteration n
$N_{com,j}$	Number of commercial customers at substation j
$N_{EV,j}$	Estimated amount of EVs connected to substation j
N_{EV}^{REGAL}	Total number of estimated EVs
$N_{EV,m}^{REGAL}$	Estimated number of EVs in cell m
$N_{EV,res}^{ratio}$	Estimated amount of EVs per residential customer
$N_{res,j}$	Number of residential customers at substation j
N_{res}^{REGAL}	Total number of estimated residential customer
$N_{res,m}^{REGAL}$	Estimated number of residential customers in cell m
$P_c^{EV}(t)$	Active power consumption for the EV charging profile c at time t
$P_{com,j}(t)$	Active commercial power consumption at time t
$P_{i,j}(t)$	Active power consumption for customer i connected to substation j at time t
$P_{j,n}^{max,\text{EV}}$	Active peak power at substation j at iteration n with EV integration
$P_{j,n}^{max,\text{No EV}}$	Active peak power at substation j at iteration n without EV integration

P^{max}_{REGAL}	Aggregated estimated peak load
$P^{max}_{REGAL,m}$	Estimated peak load in cell m
$P_{res,j}(t)$	Active residential power consumption at time t
$P^{EV}_{res,j}(t)$	Active residential power consumption at time t with EV integration
$P^{max}_{res/tot}$	Aggregated peak load, either residential or total depending on context
$P_{tot,j}(t)$	Active total power consumption at time t
$P^{EV}_{tot,j}(t)$	Active total power consumption at time t with EV integration
$S^{Ellevio}_{j}$	Rated capacity for substation j
$S^{Ellevio}_{res}$	Total residential capacity
S^{REGAL}_{res}	Total estimated residential capacity
$S^{REGAL}_{res,m}$	Estimated transformer capacity in cell m
$U_{a,b,c}$	Voltage at phase a, b, c
U_{avg}	Average voltage U
U_h	Denotes the voltage amplitude at harmonic order h
$\Delta P_{j,n}$	Active power peak change at substation j at iteration n
$\mu_{\Delta P,n}$	Mean value of active power peak change at iteration n
$\mu_{res,j}$	Residential capacity share at substation j
$\overline{\mu}_{\Delta P}$	Global mean value of active power change
$\overline{\mu}_{k_{1,2}}$	Global mean value of the Velander constants k_1 and k_2
$\sigma_{\Delta P,n}$	Mean value of active power peak change at iteration n
$\overline{\sigma}_{\Delta P}$	Global standard deviation of active power change
$\overline{\sigma}_{k_{1,2}}$	Global standard deviation of the Velander constants k_1 and k_2
$MAPE_P$	Percentage deviation of peak load
$MAPE_S$	Percentage deviation of capacity
THD_U	Denotes the total harmonic distortion for voltage U
VUF	Denotes the voltage unbalance factor [-]
$year$	Set of all hours over a year

Contents

List of Figures

List of Tables

1

Introduction

1.1 Background

The transportation sector is a major contributor to greenhouse gas emissions, and one key strategy to reduce these emissions is the adoption of electric vehicles (EVs) [1]. In Europe, transportation accounted for 25% of total greenhouse gas emissions, with 70% of that coming directly from transportation on the road. In 2021, the European Union (EU) introduced the "Fit for 55" proposal, a key milestone aimed at making Europe climate-neutral by 2050 and ensuring that all new cars sold by 2035 are zero-emission [2]. Electric vehicles (EVs), including plug-in hybrid electric vehicles (PHEV), battery electric vehicles (BEV), and other vehicles with electric charging capability, accounted for 13% of the total vehicle fleet in Sweden, with their number increasing by 18% in 2023. In contrast, EVs represented only 3.9% of the vehicle fleet across the rest of Europe [3, 4]. As the number of EVs increases, studies show that their charging adds load to residential and distribution grids, potentially impacting rated power, causing voltage variations, injecting harmonics, and creating other power quality issues at the connection point [1, 5].

The Reference Electricity Grid Analysis (REGAL) model consists of a synthetic low-voltage grid designed to meet the national grid requirements in Sweden, with high geographical resolution. It supports the integration of various load types, including average load profiles for households, apartments and EVs. The REGAL model consists of grid cells, each measuring an area of $1\,\mathrm{km}^2$, with a total of approximately 105.000 cells. The longest cable is used to estimate the largest voltage drop both with and without EV integration, as the lowest voltage in the network is assumed to occur at the end of the longest cable, not necessarily where the load is highest. The purpose of the REGAL model is to estimate the needed hosting capacity for each grid cell, based on the residential demand [6].

Ellevio is one of the largest grid owners in Sweden, that owns the electricity grid in seven different counties in Sweden. Ellevio also provides electricity network services, connections for wind and solar power plants and solutions for charging EVs. Ellevios grid is 83.6 thousand kilometres long and delivered 24.2 TWh in 2023 of electricity through their grid. Ellevios have almost 1 million costumers where 86 % of them are households [7].

1.2 Literature review

A significant body of research has explored the impact of EV charging on the LV grid, primarily using theoretical or simulation-based approaches. These studies often rely on statistical models, synthetic load profiles or scenario-based simulation to estimate the consequences of rising EV penetration on transformer ageing, cable and transformer loading, and voltage and frequency stability. Several notable examples from the literature are outlined below:

In Barros et al. [8], the authors analysed the transformer ageing factor for various EV penetration levels during summer and winter. A probabilistic framework based on Monte Carlo simulation to evaluated to estimate the transformer's hottest-spot temperature and corresponding ageing factor. The study utilized real residential demand data obtained from grid measurements, along with EV charging profiles derived from several UK-based projects. The result indicated that during summer, a 50% penetration level of long-ranged EVs led to an ageing factor of 5.2. This means that the transformer aged 5.2 times higher under normal operations, for example, 1 h of operation correspond to 5.2 h of ageing. Similarly, findings were reported by Jain et al. [9], who showed that increasing EV penetration significantly reduced the transformer's lifespan. However, with the implementation of a reactive power controller and compensation strategies, transformer ageing was improved, resulting in a lifespan extension of nearly 50%. This suggests that performance improvements can be achieved through control-based solutions without requiring substantial infrastructure upgrades.

In Polat et al. [10], the authors analysed the impact of EV charging in residential LV grids, focusing on voltage drops, transformer overloading, power losses and voltage unbalances. The study created 1000 simulated charging profiles based on statistical models, based on arrival and departure times corresponding to typical work hours. Three scenarios of EV penetration, 10%, 30% and 50%, were analysed using load flow analysis performed with forward-backward sweeping methods. The load flow analyses evaluated the LV grid's performance in terms of losses, loadings and voltage magnitudes. The findings revealed that with a 50% EV penetration, the probability of voltage violations increases by 25%. However, the probability of transformer overloading only increased by 8.5%.

In Aguilar et al. [11], the authors investigated the impact of EV charging stations on the distribution transformers and feeders within the electrical grid at California State University Northridge. The study evaluated both residential and commercial EV charging using a detailed simulation model, with various scenarios with different penetration levels and charging strategies assumed to draw 10 kW. The result showed that with 10% EV penetration, two lines and one transformer experienced overloading at peak hours. At 25% the stress increased significantly, with 18 lines and three transformers exceeding their transformer capacity. These findings highlight the challenges a relatively small penetration of EV adoption can impose.

In Zaferanlouei et al. [12], a Norwegian case study presented in, the authors analysed a small section of the distribution grid with roughly 860 customers connected to 32 medium-low voltage transformers rated at 22/0.23 kV. The study used the total active and reactive power consumption data for the area, with individual customer loads where estimated based on the total power share for each transformer. EV charging profiles were synthetically created based on the mean and standard deviation of the daily driving distance, arrival and departure time, also different types of charger power ratings. The impact of various charging strategies such as uncontrolled and smart charging, was evaluated. The analysis included voltage drop at roughly 1000 nodes and the load of both cables and transformers. Resulted showed that with uncontrolled charging the power flow exceeded both the cable and transformer capacities, also the voltage drop exceeded grid requirements. However, When smart charging was implemented with grid constraints, neither cables nor transformer capacities were exceeded, and the voltage level remained within acceptable limits.

In Kerdphol et al. [13]. The authors propose a synthetic inertia method using Vehicle-to-grid (V2G) technology via bidirectional chargers, enabling EVs to contribute to grid stability while maintaining a battery state of charge (SOC) above 80%. The approach involves the implementation of a centralised control system to coordinate and regulate the support of synthetic inertia in real-time. The results indicate that V2G-enabled EVs can provide immediate synthetic inertia during disturbance, effectively counteracting load fluctuations and variability from renewable energy resources. The study demonstrates that system frequency can be maintained within acceptable limits, highlighting V2G as promising for enhancing frequency stability in renewable-dominated power systems.

In Hungbo et al. [14], the authors evaluated the impact of EVs in LV grids using a probabilistic framework derived based on real EV charging data. Monte Carlo simulations were used to evaluate two grid models: one without photovoltaic (PV) integration and one with PV generation. The results indicate that, without PVs, transformer loading increased by 20% under high EV penetration. However, when V2G was implemented the increase in transformer loading was limited to only 1%, highlighting its potential for load balancing. Additionally, the inclusion of PV generation reduced transformer loading by 24%, demonstrating the beneficial impact of PVs in reducing grid stress associated with EV adoption.

In Chandra et al. [15]. The authors investigated the optimal solar-powered EV charging stations within radial networks, with the primary objective of minimizing cost. The study evaluated three charging strategies: direct charging, smart charging and smart V2G. The analysis focused on maintaining voltage stability within acceptable limits and evaluating the impact of the charging methods on transformer ageing and power losses. The results demonstrated that smart charging and V2G methods reduced power losses by approximately 14% and 22%, compared to direct charging. Furthermore, the transformer ageing factor was reduced by nearly

12% with the implementation of smart V2G, suggesting a potential extension of transformer lifespan. Additionally, the V2G strategy contributed to improved voltage stability at critical buses by reducing dips.

1.3 Aim

This thesis aims to evaluate the impact of increasing electrification of the passenger car fleet on the existing LV grid by comparing the synthetic REGAL model to real grid data provided by Ellevio. The study focuses on a 100% EV penetration scenario to evaluate how residential EV charging affects the local grid performance and whether the substation limits are exceeded. Furthermore, the accuracy and applicability of the REGAL model are evaluated. Unlike previous studies that primarily rely on simulations and or statistics, this thesis integrates real load measurements and EV charging data to provide a more realistic analysis and data-driven analysis of grid performance under widespread EV penetrations.

Based on the overall aim of the thesis, the following research questions have been expressed:

1. Can the REGAL model be used for grid planning in Ellevio's grid, and If so, under what conditions?
2. To what extent is the REGAL model's estimated peak power demand accurate in areas with a predominately residential share, and how is this accuracy influenced by customer composition, electric vehicle ownership and residential density?
3. How does 100% EV penetration influence EV grid loading, as evaluated from two perspectives: (i) the calculated increase in peak load, and (ii) the comparison between calculated peak loads and peak demands estimated by Velander's formula?

1.4 Limitations

The following limitations will be used in this project:

- The analysis is focused on LV grids, defined as grids with nominal voltage levels of 0.4 kV.
- The focus is exclusively on residential EV charging.
- Only a small part of Ellevios grid will be used, where different amounts of EVs per residential customer will be used for analyses. Where a few areas with different population densities will be investigated.
- Only passenger cars are considered in the demand analysis, other types of vehicles are excluded.
- Grid planning analysis is focused on evaluating power limitations in substations, other aspects such as voltage quality or grid economics are not considered.

2
Theory

2.1 Grids

This section provides an overview of the Swedish grid structure, including the necessary components. It will also discuss key topics such as grid requirements, system strength, hosting capacity, and the integration of Distributed Energy Resources (DERs).

2.1.1 Swedish grid structure

The Swedish grid is divided into three categories: the transmission grid, the regional grid, and the local grid. The combination of the regional and local grids is referred to as the distribution grid. The transmission grid can be compared to a highway, where large amounts of energy are transferred with minimal losses. The regional grid resembles the national road system, connecting different cities across the country. The local grid functions like the road system within a city, distributing energy to various consumers [16].

This section provides an overview of the different types of grids in Sweden, explaining their structure, voltage levels, and roles in electricity distribution. It also introduces the major electricity companies that operate within these networks.

- **Transmission grid:** The Swedish transmission grid operates at voltages between 220 kV and 400 kV. Svenska Kraftnät (SvK) is the system operator responsible for managing the transmission network and ensuring the balance between electricity production and consumption. Electricity suppliers in Sweden are legally required to provide enough power each hour to meet the demand. To handle any imbalances between forecasted and actual consumption or production, various balancing service providers adjust the supply or demand. The transmission network is designed to transport electricity efficiently over long distances while minimizing system losses [16].
- **Regional grid:** The regional grid typically operates at voltages between 30 kV and 130 kV, connecting to the transmission grid, local grids, various production facilities, and high-demand loads such as industries. The majority of the regional grids or Distribution System operators (DSO) are owned by three companies: E.ON Elnät Sverige, Vattenfall Eldistribution, and Ellevio [16].
- **Local grid:** The local grid typically operates at voltages between 0.4 kV and 20 kV. It is responsible for distributing electricity to end users such as

households, small businesses, and local services. In this context, voltages up to 1 kV are considered low voltage (LV), while voltages between 1 kV and 20 kV fall under medium voltage (MV). The low voltage grid represents the final stage of electricity distribution, typically connecting consumers through 230/400 V systems. Additionally, small-scale electricity production such as photo voltaic (PV) is also connected at this level [16].

- **Electric companies:** 170 different companies are related to the local and regional grid, where the majority of the companies have a strong connection to the municipality. The three biggest companies E.ON Elnät Sverige, Vattenfall Eldistribution, and Ellevio, provide more than half of electricity to the consumers [16].
- **Concession Areas:** Sweden's electrical grid is divided into approximately 300 concession areas, each assigned to a grid operator. The grid operator holds a monopoly and has the obligations to build, operate, maintain the network and connect new customers. This means the grid operator is responsible for planning and ensuring grid capacity, including adapting to future needs. This framework is regulated by the Swedish Electricity Act (1997:857) and supervised by Energimarknadsinspektionen (Ei) [17, 18].

2.1.2 Components in the grid

This part explains the different components of the electrical power grid and its main applications.

- **Substations** are used to maintain the functions of transformers and minimize losses. The key components are:
  1. **Transformers** primary function in the electrical power grid is to adjust AC voltage levels, either stepping up or stepping down, while maintaining the same frequency and power balance. In particular, distribution transformers step down the voltage to levels suitable for end-users, such as commercial and residential loads [19].
  2. **Circuit breakers** has the same function as a switch for the grid. During faults or disturbances, the circuit breaker switches off and protects the rest of the system, this can be done manually or automatically [20].
  3. **Relays** are designed to measure quantities such as voltage and current to detect unwanted conditions, such as overcurrent or overvoltage. When an unwanted condition is detected, the circuit breaker is triggered to switch off the circuit [20].
  4. **Busbars** enable efficient power distribution by serving as central nodes that connect multiple circuits with minimal losses. Typically made of copper or aluminium, they enhance electrical reliability by reducing resistance and improving conductivity. Commonly used in substations, busbars support load management and streamline switching operations, ensuring operational flexibility [21].
- **Power lines and cables:** There are multiple techniques to transport electricity, the main techniques are: Overhead lines, underground cables and sea cables. The choice of techniques has different purposes and consequences

[22]. The conductors of the lines and cables are typically made of copper or aluminium, both of which provide good electrical conductivity and mechanical strength [23].

1. **Overhead lines:** The transmission grid primarily consists of overhead lines. In the regional grid, they are used in open landscapes, but also provide connection between different urban areas. To ensure reliable operation, overhead lines are installed along line corridors, and strips of land are cleared of tall vegetation to reduce the risk of interference. In the local grid, such corridors do not exist, which increases the risk of falling trees and weather-related disturbances. While Overhead lines are cost-effective and relatively easy to maintain, they are more vulnerable to damage and environmental factors and have a significant visual impact on the landscape [24].
2. **underground cables:** In regional grids, underground cables are generally not used over long distances due to technical limitations but can be used over short distances, especially in densely populated areas where overhead lines are impractical. In local grids, underground cables are more common, particularly in urban areas, cities or forested areas where falling trees can cause damage. The key advantages are the protection from weather-related damages and improved aesthetics. However, they involve installation costs and are more difficult and costly to maintain [23, 25].
3. **Submarine (Sea) cables:** Sea cables share many of the advantages of underground cables, particularly in terms of protection and durability. They are primarily used to connect regions separated by bodies of water. This cable is armoured to withstand mechanical stress and environmental impacts, making it a reliable solution. The main drawback is that faults can be time-consuming and costly to locate and repair [26].

2.1.3 Grid requirements

The Swedish grid follows multiple standards and requirements regarding voltage magnitudes, frequency, and harmonic content. One of the most important standards is EN 50160, which applies to low and medium-voltage grids. In this context, the LV range refers to phase-to-phase voltages below 1 kV, while the MV range covers phase-to-phase voltages between 1 kV and 35 kV. EN 50160 includes various definitions, such as:

- **Nominal voltage:** The voltage at which the system is designed to operate.
- **Voltage dip:** A sudden drop in voltage to a value between 1% and 90% of the nominal voltage, lasting between 10 ms and 1 min.
- **Voltage interruption:** When the voltage falls below 1% of the nominal voltage; interruptions can be either accidental or prearranged.
- **Harmonic voltage:** A sinusoidal voltage with a frequency that is an integer multiple of the fundamental frequency (50 Hz).
    1. **Individual:** The relative voltage amplitude U_h related to the fundamental voltage U_1, where h is the order of the harmonic.

2. **Global:** The total harmonic distortion (THD) quantifies harmonic distortion in a voltage waveform and is defined as:

$$THD_U = \frac{\sqrt{\sum_{h=2}^{\infty} U_h^2}}{U_1} \tag{2.1}$$

- **Voltage unbalance:** When the voltage magnitudes or the phase angles between the three phases are not equal.
  1. The average voltage can be calculated according to [27]:

$$U_{avg} = \frac{U_a + U_b + U_c}{3} \tag{2.2}$$

  2. Where the voltage unbalanced factor (VUF) can be calculated according to [27]:

$$VUF = \frac{|U_{a,b,c} - U_{avg}|^{max}}{U_{avg}} \tag{2.3}$$

EN 50160 specifies limits on the number of voltage dips and interruptions allowed per week or year, as well as the allowed harmonic content. Table 2.1 summarizes the most important EN 50160 requirements that electrical suppliers must follow, to ensure a consistent voltage and power quality for its end-users. However, while EN 50160 puts the minimum requirement for all European countries, TSOs or individual countries may use stricter requirements to ensure a better voltage and power quality [28].

Table 2.1: Requirements according to EN 50160

Parameter	Description
Frequency	±1% (49.5 - 50 Hz) for 99.5% of the week.
Voltage magnitude variations	±10% of nominal voltage for 95% of the week.
Short interruptions	Up to a few hundred per year (lasting up to 3 minutes).
Long interruptions	Fewer than 10 to 50 per year (longer than 3 minutes).
Voltage unbalance	Up to 2% for 95% of the week.
Harmonic content	THD < 8% (see equation 2.1)

2.1.4 System strength

The definition of system strength varies between industry and academic institutions. In power systems, it is often synonymous with short-circuit capacity (SCC). However, a more widely accepted definition is the system's sensitivity of voltage to changes in current and power flow. It can also be described as the stiffness of voltage, similar to how inertia affects frequency deviations. There are multiple definitions, but they all share a common theme: the sensitivity of the grid and its response to various events, such as disturbances or changes in power and current flow [29].

A weak grid is more susceptible to voltage instability, particularly in areas dominated by inverter-based resources (IBRs). Low system strength in these grids increases the risk of protection malfunctions, as decreased power quality can lead to challenges in maintaining protection coordination and overall grid stability [29].

2.1.5 Hosting capacity

Hosting capacity (HC) refers to the maximum additional generation or load that can be integrated into the existing grid without exceeding operational limits or causing grid violations, such as voltage levels, thermal limits and power quality requirements [30].

According to [31] a weak grid with low short-circuit current is more susceptible to voltage oscillations, especially in areas with a high concentration of DERs. Changes in production or load can cause noticeable voltage variations in such grids. As DER penetration increases, the required system strength must also increase, as the likelihood of DERs affecting voltage stability grows. As DER concentration increases, it becomes more important to improve system strengths to ensure grid stability. According to [32], it has been shown that as PV penetration increases and hosting capacity is reached, voltage variations caused by PVs, a type of DER, become more noticeable, potentially leading to voltage violations.

2.1.6 Distributed energy resources

Distributed Energy Resources (DERs) refer to a range of technologies connected to the distribution grid. These include renewable generation systems like PV panels, wind power, energy storage solutions such as batteries, and EVs. While there are various definitions of DERs, their common goal is to reduce greenhouse gas emissions and decentralize energy production. Additionally, new business models are being explored in which prosumers, or consumers who both generate and consume energy, are integrated into the grid, shifting away from traditional centralized production to more distributed, flexible energy markets [33].

Inverter-based resources (IBRs) are a subset of DERs that use inverters to connect to the AC grid, converting DC to AC. These include Type 3 and Type 4 wind turbines, solar PVs, and battery energy storage systems. The main differences between IBRs and traditional power sources lie in their dependence on power electronics, which makes them more sensitive and results in lower fault currents [34].

There are studies that show that Several studies highlight the potential benefits of DERs. For example, they can reduce power losses [35], provide voltage support during grid faults [36], and increase the hosting capacity of distribution networks for PV integration [37]. However, other studies indicate that DERs can also introduce challenges, such as voltage and frequency instability, voltage dips, overvoltage events, extended disturbances, overall power quality issues, and damage of different equipment due to reverse power flow [36, 38, 39].

These results differ when analysing DERs because they depend on several factors, such as the penetration level of the technology and how it is implemented in the grid.

2.2 Topology of distribution and local grid

The Local and distribution grid can be configured using several grid topologies, which determine how cables and lines are connected to ensure electricity delivery. The three main topologies used in distribution and low voltage grids are: radial, ring (loop) and meshed topology.

Radial topology is characterized by a tree-like structure in which loads are connected to the supply source, via a single unidirectional path. This configuration is widely used in residential areas or regions with small-scale industries, due to its simplicity in design and cost-effectiveness. However, its main limitation is its vulnerability to faults and voltage drop issues [40].

Ring topology, also referred to as loop topology is arranged such that each node is connected to two others. Forming a closed loop. This enables bidirectional power flow, making it more reliable during faults in the ring. While this topology offers fault tolerance compared to radial systems, it introduces increased complexity and maintenance challenges. Ring topologies are most common in transportation systems and industrial facilities [41].

Meshed topology involves multiple connections between. This configuration provides high reliability, fault tolerance and voltage stability. Meshes grids are typically implemented in critical infrastructures and large-scale industrial complexes where operation is essential. However, these benefits come with an increased investment cost, increased complexity and maintenance challenges [41].

3
Methods

This section describes the methodological framework used to evaluate the accuracy of the REGAL model under 100% EV penetration, using real grid data from Ellevio. The overall process is illustrated in the flowchart in Figure 3.1, Which was structured into three main phases: Input & Preprocessing, Modelling & Analysis and Evaluation & Insights.

The methodology begins with the selection of areas. Based on predefined criteria such as residential share and area size. Data collection was then implemented by using three main sources: measured data from Ellevio, estimated data from REGAL and approximately 170 distinct EV charging profiles. The collected datasets were subjected to preprocessing, including filtering and aggregation steps, to ensure consistency and preparation for analysis.

In the Modelling & Analysis phase, EV charging profiles were integrated with load estimations from REGAL and compared with measured data. In parallel, substation data from Ellevio, including maximum peak loads and rated substation capacities were used. Two REGAL scenarios are used: one with 0% EV penetration and one with 100%, allowing for a direct comparison between estimated peak loads and capacities under different penetration levels. These comparisons enable an evaluation of the REGAL model's accuracy and the additional load stress introduced by electric vehicle (EV) charging on the LV grid.

Finally, the Evaluation & Insights phase quantifies the model's accuracy using the Mean Absolute Percentage Error (MAPE). Additionally, a grid impact analysis was performed through two perspectives: The observed load increase due to EV charging and a Velander Constant Analysis, which examines the load diversity across different areas.

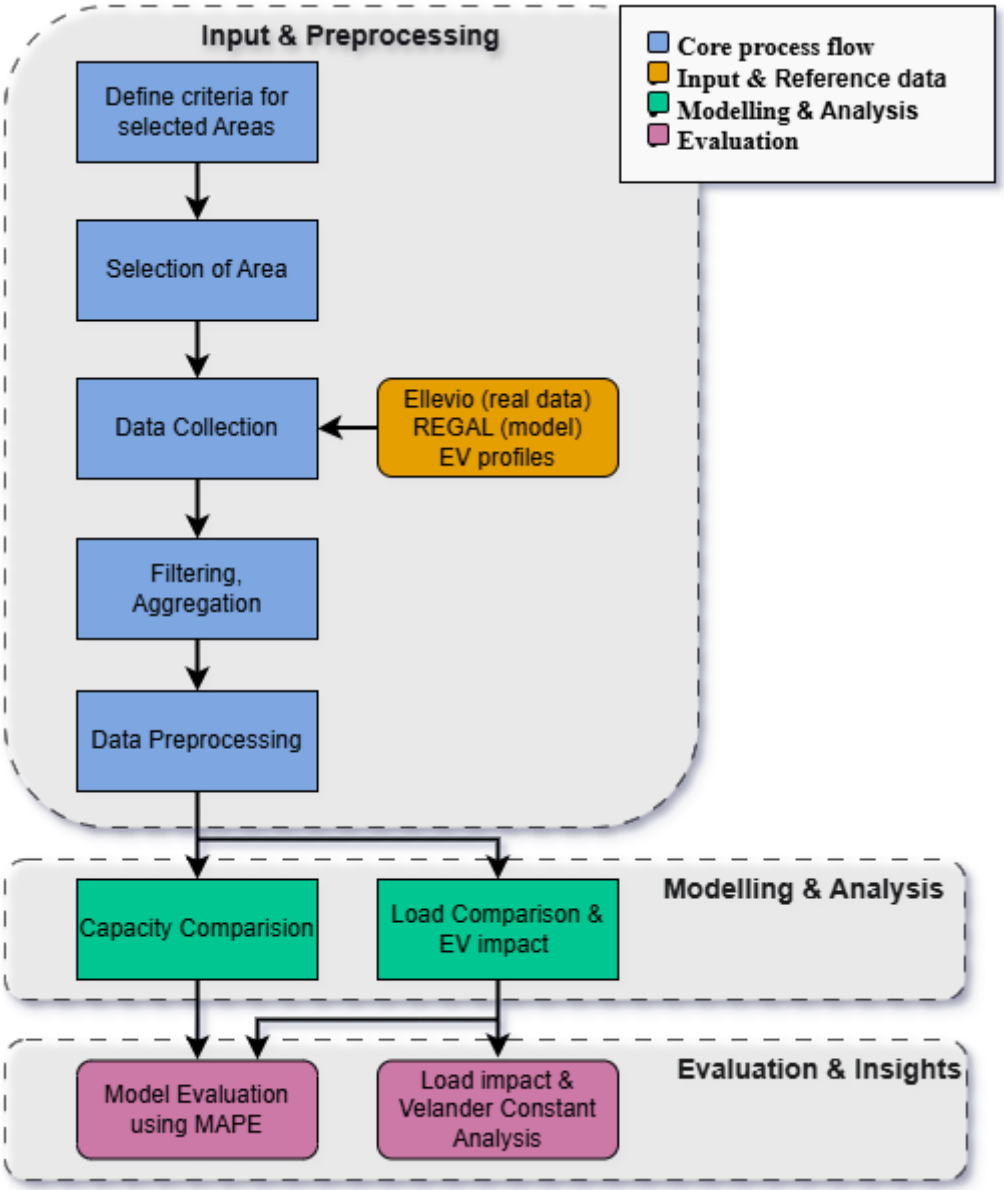

Figure 3.1: Overview of the methodology.

3.1 REGAL model

The Regal model considers only residential customers, excluding other types of grid load such as commercial load. There were multiple load profiles corresponding to different customer types. Within a residential category, customers were classified as either houses or apartments, each containing a variety of distinct load profiles and subcategories. The yearly energy consumption of all houses and apartments within a grid cell was used to calculate the corresponding peak power using Velander's formula in Equation 3.11. The estimated peak power from Velander's formula was then used to size the transformers within each grid cell, assuming that all transformers in the same grid cell have identical capacities.

The model then combines the created synthetic grid with residential load profiles and EV charging that were added to the residential load. Finally, it analyses whether the additional load from EV charging causes transformer violations, defined as when power demand exceeds transformer capacity [6].

3.2 Criteria for selecting areas

The REGAL model divides the Swedish grid into cells of $1\,\mathrm{km}^2$ in size, estimating the number of transformers and demand for each cell. To compare actual data with the REGAL model, several areas were chosen for comparison

To enable the comparison, actual data from the DSO company Ellevio were obtained. This data included multiple parameters from transformers managed by Ellevio. The energy consumption data covered a full year with a resolution of one hour, totalling 8760 hours, which allowed for the analysis of seasonal variations in load demand.

In the REGAL model, the accuracy when analysing individual cells of $1\,\mathrm{km}^2$ in rural areas showed an average deviation of 44.5 % from the actual hosting capacity. When analysing municipality areas in Sweden with an electrical connection, the average deviation from the actual capacity was $\pm 10\,\%$, covering an area of a municipality in Sweden [6].

Although the REGAL model showed a high deviation when individual cells were analysed it was acceptable at the municipality level in Sweden. To improve REGALs reliability compared to the 44.5% deviation at smaller scales, an area of at least $5\,\mathrm{km}^2$ was selected for analysis. This decision was driven by the need for statistical significance, a larger area provided a broader sample size that better captured variations in demand and capacity. A smaller area might not have captured enough variations in the total demand and capacities. Therefore, selecting a larger area provided robustness and reliability for the analysis.

The REGAL model is based on residential loads and the integration of EVs connected to houses and apartments. Therefore, the majority of customers in the selected area had to be residential. Specifically, the number of residential customers had to make up at least 85 % of the total customer base in the area. A high residential share was essential for statistical significance when comparing the REGAL model with actual data, as commercial loads could introduce noise into the analysis. Additionally, since EV charging profiles are directly linked to residential customers, a lower residential share would have increased the influence of commercial loads, further adding noise to the results.

In summary, for an area to be considered interesting for further analysis, it must meet the following criteria:

Table 3.1: Criteria for Selecting Areas for Further Analysis

Criteria	**Requirements**
Minimum area size	$5\,\mathrm{km}^2$
Residential customer share	85 %

3.2.1 Selected areas for cases

Area 1: is a typical urban town in Sweden, that is dominantly made of houses with a few schools and grocery stores. The area also includes a ski facility and a separate area for commercial purposes. The population is roughly 5400, covering an area of $6\,\mathrm{km}^2$, resulting in a population density of approximately $900\,\mathrm{People/km}^2$. The majority of the customers in this area were residential, accounting for about 90 % of the total 2250 customers connected to 47 substations (see Appendix A.1 for a detailed customer distribution per substation). However, in terms of energy usage, residential load represent approximately 70% of the total annual energy consumption. According to REGAL, the estimated number of cars per residential customer was 1.24.

Area 2: is a typical urban outside one of the bigger cities in Sweden, that is mostly dominated by made of houses with a few schools, grocery stores and two separate areas for commercial purposes. The population is roughly 8400, covering an area of $6.5\,\mathrm{km}^2$ resulting in a population density of approximately $1300\,\mathrm{People/km}^2$. The majority of the customers in this area were residential, accounting for about 88 % of the total 3950 customers connected to 89 substations (see Appendix A.2 and A.3 for a detailed customer distribution per substation). However, in terms of energy usage, residential load represent approximately 64% of the total annual energy consumption. According to REGAL, the estimated number of cars per residential customer was 1.1.

Area 3: is the densely populated urban area outside one of the biggest cities in Sweden, which is mostly made of houses and apartments. The Area has many schools, grocery stores and commercial activities that are more similar to a bigger city. The population is roughly 24000, covering an area of 8 km^2 resulting in a population density of 3000 People/km^2. The majority of the customers in this area were residential, accounting for about 86 % of the total 12700 customers connected to 88 substations (see Appendix A.4 and A.5 for a detailed customer distribution per substation). However, in terms of energy usage, residential load represent approximately 52% of the total annual energy consumption. According to REGAL, the number of cars per residential customer was lower at 0.66, compared to Areas 1 and 2.

3.3 Data Source and Processing

This section describes the different parameters and how they were used in the analysis, the parameters were obtained from the REGAL model and different software's from Ellevio.

Table 3.2: Parameter description obtained from Ellevio and REGAL

Parameter	Source	Description
Customer type	**Ellevio**	Classification of customers as either residential or commercial, denoted as "res" or "com".
Timestamp	**Ellevio**	The specific hour t when the active energy consumption was recorded.
$P_{i,j}(t)$	**Ellevio**	Hourly active power consumption for customer i connected to substation j at time t, measured in kWh/h, representing real energy use.
Customer ID	**Ellevio**	Each customer in the grid has a unique assigned ID.
Substation ID	**Ellevio**	Each substation j in the grid has a unique assigned ID.
Secondary voltage	**Ellevio**	Voltage rating on the secondary side of the substation, measured in kV.
$S_j^{Ellevio}$	**Ellevio**	Capacity of substation j, measured in kVA.
Geographical coordinates	**REGAL**	Location of each 1 km^2 cell, represented by the south-west corner coordinates.
$N_{EV,m}^{REGAL}$	**REGAL**	Estimated number of EVs per cell m, based on the REGAL model.

Parameter	Source	Description
$N_{res,m}^{REGAL}$	**REGAL**	Estimated number of residential customers per cell m.
$S_{res,m}^{REGAL}$	**REGAL**	Estimated transformer capacity in cell m, measured in kVA.
$P_{REGAL,m}^{max}$	**REGAL**	Estimated residential peak load per transformer in cell m, expressed as a percentage of transformer capacity.
$P_c^{EV}(t)$	**REGAL**	The c-th EV charging profile. 170 unique profiles representing average energy use in 10-minute intervals over a year, in kW h per 10 minutes.

The selected area was required to meet the criteria in Table 3.1. The substations within the area were obtained using a map-interface software from Ellevio, and only those substations with a secondary voltage rating of 0.4 kV were chosen, as this voltage rating is used for residential customers. The number of residential and commercial customers connected to each substation denoted as j, was determined by filtering customer IDs based on their type and counting the unique IDs separately for residential and commercial categories. From this process, the parameters $N_{res,j}$ and $N_{com,j}$ were obtained.

The total residential load was obtained from Ellevio's databases by aggregating the hourly active energy consumption of all residential customers i connected to the same substation ID j. A similar approach was applied to commercial loads, resulting in the residential and commercial load profiles, $P_{res,j}(t)$ and $P_{com,j}(t)$, over a yearly period hourly time steps. Since most residential loads, such as heating, electronics and lightning are mainly resistive, their reactive power demand was expected to be low. Thus, a power factor close to 1 was assumed for residential customers at 0.4 kV, and their reactive power impact was considered negligible. The same assumption was made for small commercial customers connected to the LV grid, as their typical loads, such as lightning and office equipment, were mostly resistive. As shown in Table 3.1, residential customers make up at least 85 % of the total customer base. Even if the power factor for commercial customers were slightly lower, the limited share ($\leq$ 15%) would result in a negligible impact on the grid's overall reactive power demand.

Substation-specific information was obtained from Ellevios databases, which describe different attributes of individual substations. From these databases, the substation capacity $S_j^{Ellevio}$ was extracted for each substation j. Additionally, the selected cells from REGAL were determined by the actual geographical coordinates (longitude and latitude) of the substations identified in Ellevio's databases. The following parameters were obtained for each selected cell seen in table 3.2, where these parameters provided a base for further analysis for the selected areas.

3.4 EV load profiles for substations

Based on the parameters from the section on 3.3 Data Source and Processing, EV load profiles were created by combining relevant data from REGAL and Ellevio. The total number of EVs in the selected area was estimated by aggregating the number of EVs $N_{EV,m}^{REGAL}$ from each cell m, resulting in the parameter N_{EV}^{REGAL}. A similar procedure was applied to the residential customers $N_{res,m}^{REGAL}$, which resulted in the parameter N_{res}^{REGAL}. It was assumed that all cars in the selected areas were fully electrified, 100% of all vehicles were EVs. Existing EVs connected to the grid were not considered, as their demand was assumed to be included in the base load. Using these parameters, the ratio of EVs per residential customer was determined, along with the estimated number of EVs assigned to each substation j, calculated as:

$$N_{EV,res}^{ratio} = \frac{N_{EV}^{REGAL}}{N_{res}^{Est}} \tag{3.1}$$

$$N_{EV,j} = \lceil N_{EV,res}^{ratio} \cdot N_{res,j} \rceil \tag{3.2}$$

The parameter $N_{EV,j}$ in Equation 3.2 represent the estimated amount of EVs per substation, rounded up to the nearest integer. The term $N_{res,j}$ represents the actual number of residential customers connected to substation j. The ratio $N_{EV,res}^{ratio}$ represented the number of EVs per residential customer and was considered to be uniformly distributed across the selected area. This meant all residential customers were assumed to have an equal probability of owning an EV, regardless of which substation they were connected to. This assumption was considered reasonable, as each area had at least 2000 residential customers, with some exceeding 10000. With such large customer bases, small variations in EV ownership among individual households were expected to average out. Additionally, due to the lack of information on EV ownership data at the customer level, using a uniform distribution provided a statistically justified approach for the estimation of EV penetration at the substation level.

To generate the EV charging profile $P_c^{EV}(t)$, the original 10-minute resolution charging data was first aggregated into 1-hour intervals by summing all 10-minute values within each hour. After this aggregation, charging profiles were assigned to each substation through a random selection process. Specifically, for each substation j, $N_{EV,j}$ charging profiles were randomly selected from the 170 available EV profiles. This approach ensured that the assigned profiles captured a realistic variety of individual charging behaviour. Finally, the selected EV charging profiles were aggregated per substation, resulting in the total EV charging demand for each substation j, which is expressed as:

$$P_j^{EV}(t) = \sum_{c \in C_j} P_c^{EV}(t) \tag{3.3}$$

Where C_j is the set of the selected EV profiles for substation j, and P_c^{EV} denotes the c-th EV charging profile at time t. The parameter $P_j^{EV}(t)$ represents the aggregated EV profiles at substation j. From Equation 3.3 the hourly residential and combined energy consumption could be described as:

$$P_{res,j}^{EV}(t) = P_{res,j}(t) + P_j^{EV}(t) \tag{3.4}$$

$$P_{tot,j}^{EV}(t) = P_{tot,j}(t) + P_j^{EV}(t) \tag{3.5}$$

The parameters $P_{res,j}^{EV}(t)$ and $P_{res,j}(t)$ represent the hourly demand from residential customers at time t, with and without EV integration. Similarly, the parameters $P_{tot,j}^{EV}(t)$ and $P_{tot,j}(t)$ represent the total demand, with and without EV integration. Equations 3.4 and 3.5 provided a foundation for further analysis of residential load and transformer utilization in the selected areas. These formulations are necessary for understanding energy consumption dynamics and the impact of EV charging on both residential and total grid demand.

3.5 Load analysis when including EVs

3.5.1 Max load comparison

Max load comparisons were used to evaluate how much the peak demand was expected to increase due to the integration of EVs. This provided an understanding of the added stress EV charging could affect the grid during peak hours, helping to understand the potential needs for future capacity upgrades. The maximum load comparison was analysed for each substation both with and without the inclusion of commercial loads, where the change in peak load was calculated using the following equation:

$$\Delta P_{j,n} = \frac{P_{j,n}^{\text{max,EV}} - P_{j,n}^{\text{max,No EV}}}{P_{j,n}^{\text{max,No EV}}} \cdot 100\% \tag{3.6}$$

The parameter $\Delta P_{j,n}$ represents the percentage change in peak load for substation j due to EV integration at iteration n. The term $P_{j,n}^{\text{max,EV}}$ denotes the maximum peak load with EV integration, while $P_{j,n}^{\text{max,No EV}}$ represents the maximum peak load without EV integration. The equation compares the difference between these two values and calculates the percentage change.

Following the load change calculations, the average and standard deviation load change were calculated for a selected area. These were calculated using the following equations:

$$\mu_{\Delta P,n} = \frac{1}{J} \sum_{j=1}^{J} \Delta P_{j,n} \tag{3.7}$$

$$\sigma_{\Delta P,n} = \sqrt{\frac{1}{J} \sum_{j=1}^{J} \left(\Delta P_{j,n}, -\mu_{\Delta P,n}\right)^2} \tag{3.8}$$

The parameters $\mu_{\Delta P,n}$ and $\sigma_{\Delta P,n}$ in Equation 3.7 and 3.8 represent the mean and standard deviation of the load changes at iteration n.

It was observed that the results varied depending on the specific iterations used when randomly selecting EV charging profiles. Due to this sensitivity, it was decided to perform multiple iterations and compute the mean and standard deviation for each iteration. Using multiple iterations and calculating the global average and standard deviation, provided a more robust and representative outcome by reducing the noise introduced by random variations in the EV charging profiles.

The mean and standard deviation values, and the mean of the standard deviations across multiple iterations N, were calculated as follows:

$$\overline{\mu}_{\Delta P} = \frac{1}{N} \sum_{n=1}^{N} \mu_{\Delta P,n} \tag{3.9}$$

$$\overline{\sigma}_{\Delta P} = \frac{1}{N} \sum_{n=1}^{N} \sigma_{\Delta P,n} \tag{3.10}$$

The parameter $\overline{\mu}_{\Delta P}$ in Equation 3.9 describes the global load change calculated after N iterations. Similarly, the parameter $\overline{\sigma}_{\Delta P}$ Equation 3.10 calculate the global standard deviation, describing the typical variations across N iterations.

3.5.2 Calculations of Velander's constants

Velander's constants are commonly used in grid planning to estimate the relationship between max load and yearly energy consumption for different types of customers. The constants k_1 and k_2 are varied depending on the customer type and its subtype, such as residential customers living in houses with or without electric heating. These constants are used to estimate the peak demand based on its yearly energy consumption. The relationship between maximum demand and yearly energy consumption is expressed by the following equation:

$$P_{max} = k_1 \cdot E_{year} + k_2 \cdot \sqrt{E_{year}} \tag{3.11}$$

Velander's constants k_1 and k_2 were used to identify the relationship between the yearly energy consumption and the peak demand for all substations j in the selected areas for only residential customers, including the impact of EV integration. The estimation of Velander's constants was performed using multiple linear regression, where the estimated peak load for substation j was expressed as:

$$y_{res,j} = k_1^{Est} \cdot x_1 + k_2^{Est} \cdot x_2 \tag{3.12}$$

Where the parameters $x_{1,j} = E_{res,year,j}$ and $x_{2,j} = \sqrt{E_{res,year,j}}$, and the term $E_{res,year,j}$ is the annual residential consumption at substation j.

Before EVs were integrated in the selected areas, it was assumed that all customers connected to the substations shared similar load profiles, and profiles associated with houses and apartments. Established customer types were not used, instead, all customers were assumed to belong to the same residential type and subtype. This assumption excluded potential impacts such as PVs and battery storage, which may influence consumption patterns. After EV integration, the assumption remained valid, as EVs were uniformly distributed across all substations, resulting in a representative load profile that captured the impact of EV charging.

It was observed that the results from Equation 3.12 varied depending on the specific iterations used when randomly selecting EV charging profiles. Due to this sensitivity, it was decided to perform multiple iterations and compute the global mean and standard deviation for each iteration, similar to section 3.5.1.

The global mean and standard deviation for the estimated Velander's constants k_1^{Est} and k_2^{Est} were calculated as:

$$\overline{\mu}_{k_{1/2}} = \frac{1}{N}\sum_{n=1}^{N} k_{1/2,n}^{Est} \tag{3.13}$$

$$\overline{\sigma}_{k_{1/2}} = \sqrt{\frac{1}{N}\sum_{n=1}^{N}\left(k_{1/2,n}^{Est} - \overline{\mu}_{k_{1,2}}\right)^2} \tag{3.14}$$

The parameter $\overline{\mu}_{k_{1/2}}$ in Equation 3.13 describes the global mean values for the estimated Velander constants k_1 and k_2, in the selected areas. Similarly, the parameter $\overline{\sigma}_{k_{1/2}}$ in Equation 3.14 described the corresponding standard deviations, representing the typical variation across N iterations. The Velander's constants will only be true for areas that are similar to the selected areas, where the customer's consumption behaviour and charging patterns are similar to the selected areas.

3.6 Comparison between REGAL and Ellevios grid

The purpose of the comparison was to evaluate how accurately the REGAL model could represent key parameters by comparing data from Ellevio. The analysis focused on two aspects: Estimation of rated capacities and expected maximum loads. If the model proves useful under specific conditions, it is also important to evaluate its accuracy.

Evaluation Metric

To quantify the accuracy of the model, the Mean Average Percentage Error (MAPE) was used:

$$MAPE = \left|\frac{y - \hat{y}}{y}\right| \times 100\% \tag{3.15}$$

MAPE measured the average absolute percentage difference between the actual value y and REGAL's estimates $\hat{y}$, allowing comparisons between different datasets.

3.6.1 Capacity comparison

Since the REGAL model only estimated residential capacities, the rated capacities from Ellevio's grid needed to be adjusted to reflect the residential share at each substation

The residential share of each substation j, was calculated based on the ratio between the maximum load from residential and commercial customers, with and without the integration of EVs:

$$\mu_{res,j} = \frac{P_{res,j}^{max}}{P_{res,j}^{max} + P_{com,j}^{max}} \tag{3.16}$$

The terms $P_{res,j}^{max}$ and $P_{com,j}^{max}$ represent the residential and commercial peak loads in Equation 3.16. The resulting residential share $\mu_{res,j}$ was then used to scale the substation's rated capacity, to obtain the total residential rated capacity from Ellevio's data:

$$S_{res}^{Ellevio} = \sum_{j=1}^{J} \mu_{res,j} \cdot S_{j}^{Ellevio} \tag{3.17}$$

The parameter $S_{res}^{Ellevio}$ represents the total residential downscaled capacity from Ellevio, derived from the total capacity $S_{j}^{Ellevio}$ at substation j. Then REGAL estimates were calculated by aggregating the estimated capacities in each cell m:

$$S_{res}^{REGAL} = \sum_{m=1}^{M} S_{res,m}^{REGAL} \tag{3.18}$$

The MAPE between these values was calculated as follows, from the Equations 3.17 and 3.18:

$$MAPE_{capacity} = \left| \frac{S_{res}^{Ellevio} - S_{res}^{REGAL}}{S_{res}^{Ellevio}} \right| \times 100\% \tag{3.19}$$

This evaluation determines how accurately the REGAL model estimated the installed residential capacity in the selected areas. integration of EVs.

3.6.2 Maximum load comparison

To evaluate whether REGAL could capture the expected peak loads, the maximum from the residential and total loads from both REGAL and Ellevio's data were aggregated, with and without the

REGAL's total estimated residential peak demand was computed as:

$$P_{REGAL}^{max} = \sum_{m=1}^{M} P_{REGAL,m}^{max} \tag{3.20}$$

The parameter $P_{REGAL,m}^{max}$ represents the estimated residential peak load from REGAL at grid cell m. Similarly, the parameter P_{REGAL}^{max} represents the total residential peak load from REGAL in Equation 3.20. Then from Ellevio's data, both the residential and total (residential + commercial) aggregated peak load were calculated, with and without integration of EVs:

$$P_{Ellevio}^{max} = \sum_{j=1}^{J} P_{res/tot,j}^{max} \tag{3.21}$$

The parameter $P_{res/tot,j}^{max}$ represent the peak load from the residential or all customers connected to substation j. Similarly, the parameter $P_{Ellevio}^{max}$ represent the aggregated peak load from Ellevio. Lastly, the accuracy of REGAL's estimated peak demand was calculated with the values from Equation 3.20 and 3.21:

$$MAPE_{load} = \left| \frac{P_{REGAL}^{max} - P_{Ellevio}^{max}}{P_{Ellevio}^{max}} \right| \times 100\% \tag{3.22}$$

The Equation 3.22 was applied twice, once using residential peak load and once using the total peak load, to understand the influence of excluding commercial customers on REGAL's accuracy.

4
Results

This section presents the findings from the analysis of the actual grid under the integration of EVs. The results are structured to provide insights into load changes, the evaluation of Velander constants, and the accuracy of the REGAL model.

First, the impact of EV charging on load levels is evaluated by analysing residential demand and the contribution of commercial customers across various substations. A statistical analysis evaluation follows, highlighting the variability and significance of the observed load changes. Next, Velander's constants are calculated for the selected areas, discussing the influence of EVs on residential demand. This involves applying multiple linear regression to estimate peak demand based on annual energy consumption. Finally, the REGAL model is compared to measured data, with a focus on its accuracy in estimating capacities and peak loads.

4.1 Analysis on the actual grid when including EVs

In this section, there will be results that show the maximum load increase when including EVs, where a statistical analysis was used. Also the calculation of Velander's constants for the three selected Areas.

4.1.1 Load increase when including EVs

This section shows the distribution of load increase across all substations for the selected Areas when including EV charging, by using histograms. Also, a statistical analysis of the load increases with the integration of EVs.

The load increases were shown in Figure 4.1 for a specific iteration. Each subfigure in Figure 4.1a to 4.1f illustrates the load increase distribution for either residential (in blue) or all customers (in red) in Areas 1 to 3. The x-axis represents the load increase in percent, calculated according to Equation 3.6, while the y-axis shows the number of substations that fall within each percentage interval.

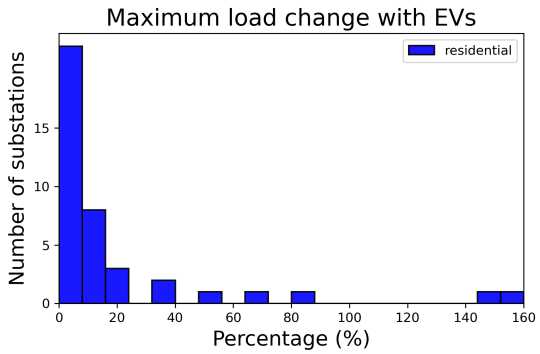

(a) Area 1: Residential load change

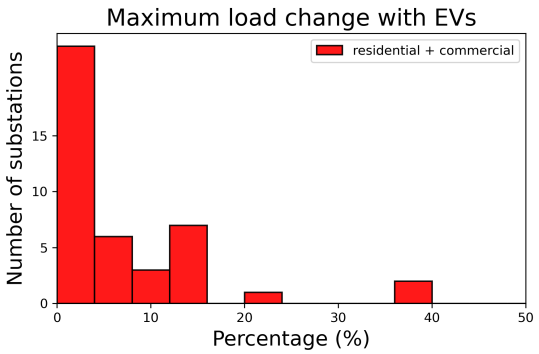

(b) Area 1: Combined load change

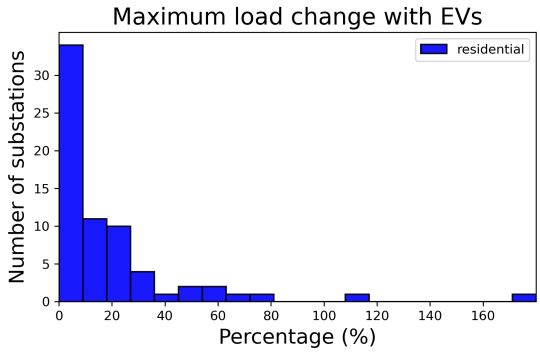

(c) Area 2: Residential load change

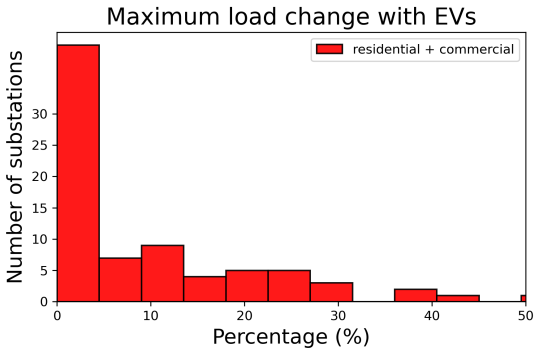

(d) Area 2: Combined load change

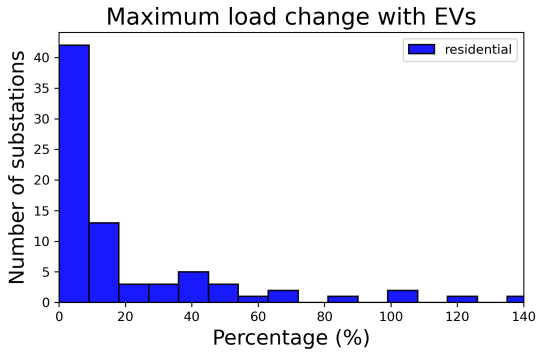

(e) Area 3: Residential load change

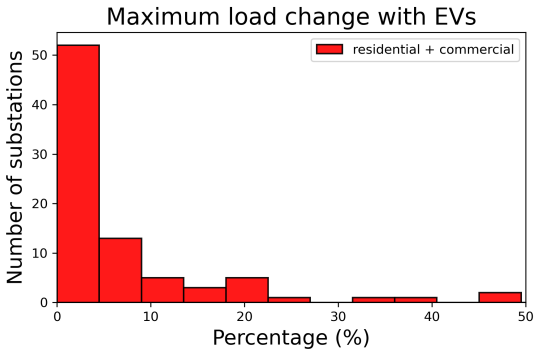

(f) Area 3: Combined load change

Figure 4.1: Histogram of load changes in the selected areas

The impact of EV integration on residential customers is shown in Figures 4.1a, 4.1c and 4.1e. In all areas, most substations experienced a residential load increase between 0 to 40%, with the mean value ranging between 13.3 to 14.7% and a standard deviation of between 18 to 19%, indicating relatively high variations between substations. A few substations experienced extreme cases, with load increases ranging from 80 to 180%. These outliers shared a common characteristic: a low average yearly energy consumption per customer compared to the rest. The affected substations had an average yearly energy consumption between 2000 and

8000 kWh per customer, where the majority of the other substations ranged between 10 000 and 17 000 kWh. A lower yearly energy consumption typically corresponds to a lower peak demand, making these substations more susceptible to load changes when EVs are integrated. The outliers did not cause any overloading, due to the fact that the substation had a low peak demand.

In contrast, Figure 4.1b, 4.1d and 4.1f show that when both commercial and residential customers were included, the increase in peak load was generally lower and more concentrated. In all areas, most substations experienced load increases between 0 and 25%, with the mean value ranging between 8.8 to 13% and a standard deviation of between 15.8 to 22%. Fewer exceeded 30%, showing a dampening effect from the commercial load which gives a more stable total load change.
Overall, the result across all three areas showed an observable increase in maximum load when adding EV charging, with residential loads being the most sensitive compared to the total loads. The lower variations showed in the histograms related to the total loads, suggest that commercial loads may stabilise the overall load profile, even with a small proportion. However, it also shows that the impact of EV charging is more sensitive to infrastructure that is dominated by residential profiles, indicating the importance of planning for substations serving only residential customers.

4.1.1.1 Statistical analysis of load changes

In Figure 4.1a to 4.1f, a few outliers that exceeded 80% were observed in the histograms related to residential loads. For all histograms, where an outlier is defined as: A value that is not centred around its mean value in this context. These deviations were primarily dominated by substations with a significantly lower average hourly energy consumption per customer over a year for all selected Areas.

This is a natural mathematical consequence when the average energy consumption is low, additional load such as charging from EVs will have a greater impact on the overall percentage change. Substations with a higher average energy consumption are therefore less sensitive to the same additional load, due to a lower relative change.

Due to the noticeable variations in the load increase distributions, both in mean, standard deviation and the existence of outliers, followed by randomly selecting EV charging profiles to the substations for each iteration. It was decided to compute the global mean and standard deviation over 1000 iterations, where the Equations 3.9 to 3.10 was used to calculate the different values, where it provided statistically robust results by averaging the different outcomes for a large number of random combinations. These results were presented in the Tables 4.1

Table 4.1: Statistics of load change for residential and total loads

Area	Residential Load		Total Load	
	$\overline{\mu}_{\Delta P}$ [%]	$\overline{\sigma}_{\Delta P}$ [%]	$\overline{\mu}_{\Delta P}$ [%]	$\overline{\sigma}_{\Delta P}$ [%]
1	14.50	19.53	14.54	21.85
2	17.17	19.92	13.14	18.53
3	16.37	21.32	8.62	15.21

The parameter $\overline{\mu}_{\Delta P}$ represents the global mean value of peak load change after 1000 iterations. Similarly, the parameter $\overline{\sigma}_{\Delta P}$ denotes the global standard deviation of peak load changes after 1000 iterations.

Table 4.1 summarises the maximum load changes observed across all substations for the different areas. The table shows the results for residential and commercial loads. The table contains the global mean and standard deviation across all substations for the three areas, based on 1000 iterations where each iteration randomly selected new EV profiles.

In the residential part in Table 4.1, the global mean value for the maximum load increase ($\overline{\mu}_{\Delta P}$) for residential customers ranged between 14.5 to 17.17%. The global standard deviation for the maximum load change ($\overline{\sigma}_{\Delta P}$) ranged from 19.53 to 21.32%, reflecting significant variations due to EV charging among substations within each area. This high variability is probably due to the presence of outliers, which will penalise the standard deviation.

Similarly in the combined part of Table 4.1, the global mean value for the maximum load increase ($\overline{\mu}_{\Delta P}$) for all customers, was generally lower and ranged from 8.62 to 14.54%. This indicates that the inclusion of commercial loads tends to dampen the overall impact of EVs. The global standard deviation ($\overline{\sigma}_{\Delta P}$) ranged from 15.21 to 21.85%, again reflecting a significant variation in load change due to EV charging.

4.1.2 Velander's constant when including EVs

This section described the calculations of Velander's constants for the selected Areas after adding EV charging, both for each iteration as well for the global mean and standard deviation over 1000 iterations. The result was calculated using Equation 3.11 to 3.14, which were used to calculate the Velander's constant k_1 and k_2 for each iteration and determine the corresponding global statistical values.

For a random iteration, the calculated Velander's constant for the selected Areas was plotted against the actual demand for the different substations. This is shown in Figure 4.2, where each subfigure shows the linear fit between estimated and actual peak loads for the substations in the three Areas.

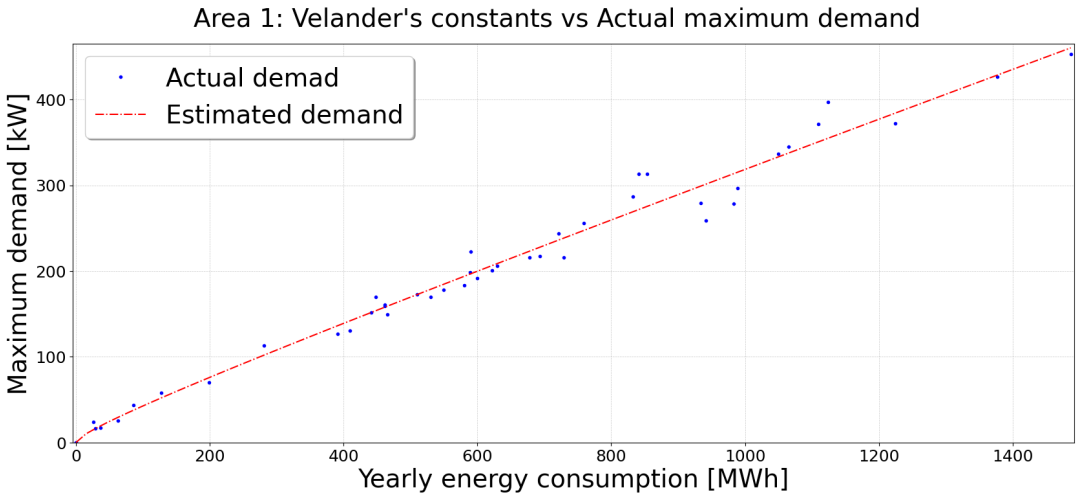

(a) Area 1: Linear fit vs actual peak demand

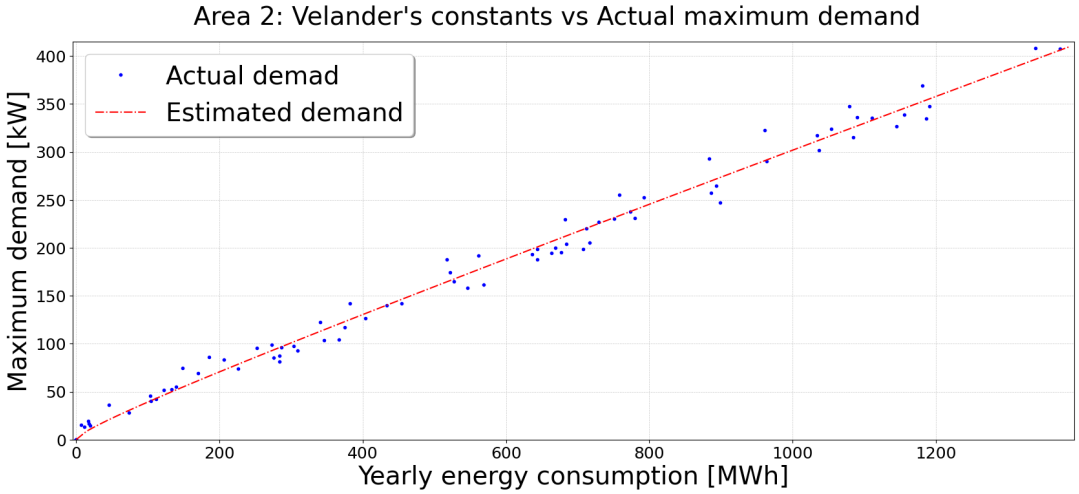

(b) Area 2: Linear fit vs actual peak demand

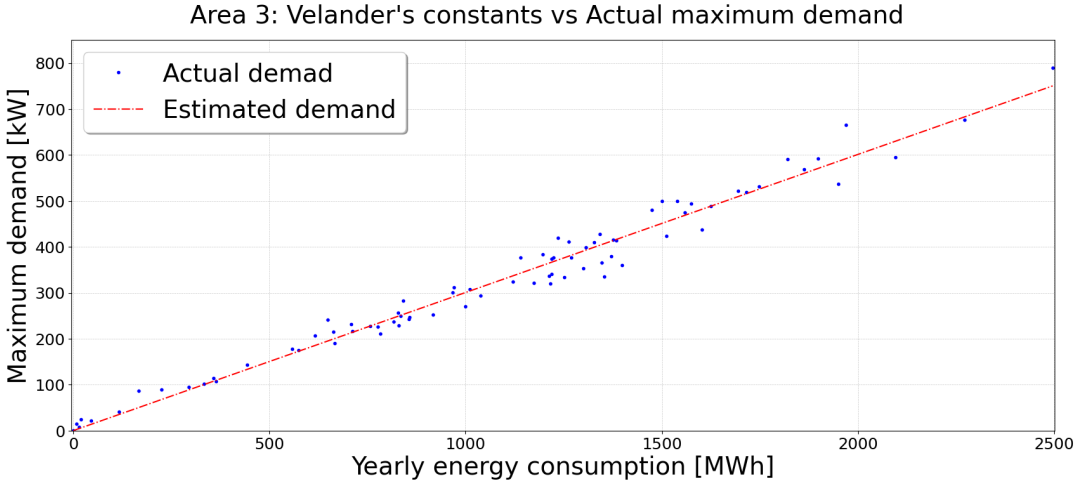

(c) Area 3: Linear fit vs actual peak demand

Figure 4.2: Multiple linear regression of actual and estimated peak demand, by using Equation 3.12

In all three areas, the calculated maximum residential demand with EVs was plotted against the yearly energy consumption, along with the estimated constants k_1^{Est} and k_2^{Est} used in Equation 3.11.

In Area 1, the estimated constants were $k_1^{Est} = 0.00028$ and $k_2^{Est} = 0.038$ as shown in Figure 4.2a, describing the relationship between the calculated peak demand and yearly energy consumption for each substation. Similarly, Area 2 had estimated constants of $k_1^{Est} = 0.00026$ and $k_2^{Est} = 0.043$, as shown in Figure 4.2b. The results in Area 1 and 2 are relatively similar, which aligns with the similarities for the customer composition, primarily consisting of single-family houses. In contrast. Area 3 showed a different behaviour, with estimated constants of $k_1^{Est} = 0.0003$ and $k_2^{Est} = 0.0007$, as shown in Figure 4.2c. This distinct characteristic of Area 3, which has a larger customer base dominated by apartments.

As shown in Figure 4.2a to 4.2c, the linear fit based on Velander's constants performs well in Area 1 and 2, with minimal deviation across the full range of yearly energy consumption between 0 to 1400 MWh. However in Area 3, Figure 4.2c, the linear fit does not perform as well compared to Area 1 and 2. The model overestimates peak demand around 500 MWh and underestimates higher energy consumption around 2000 MWh, which indicates that energy consumption and peak demand are less linear in Area 3, due to a broader yearly energy consumption up to 2500 MWh. A part of this variation can be due to the higher population density and that Area 3 is mostly apartments, compared to Areas 1 and 2.

4.1.2.1 Statistical analysis of Velander's constants

Due to the noticeable variation in Velander's constants across each iteration, caused by the random selection of new EV profiles are randomly selected for each iteration. The global mean and standard variation of the estimated constants k_1^{Est} and k_2^{Est} were calculated over 1000 iterations. This approach was chosen to ensure the statistically robust result, allowing each selected Area its representative Velander's constants. The analysis assumed that all residential customers in the selected Areas were assigned a new subtype of customers, due to the integration of EVs.

The global mean and standard deviation for the Velander's constant k_1 and k_2 were calculated according to Equation 3.13 to 3.14 after 1000 iterations, presented in Table 4.2.

Table 4.2: Velander's constants for the different Areas

Area	$\overline{\mu}_{k_1}$	$\overline{\sigma}_{k_1}$	$\overline{\mu}_{k_2}$	$\overline{\sigma}_{k_2}$
1	0.000278	0.000009	0.042019	0.007828
2	0.000259	0.000006	0.041830	0.005479
3	0.000293	0.000006	0.008783	0.006503

The parameters $\overline{\mu}_{k_1}$ and $\overline{\mu}_{k_2}$ represent the global mean values of the Velander constants k_1 and k_2, respectively, calculated after 1000 iterations. Similarly $\overline{\sigma}_{k_1}$ and $\overline{\sigma}_{k_2}$ denote the global standard deviation of the same constants, also determined after 1000 iterations. These values provide insight into the central and variability of the Velander constants in the estimation process.

The global mean value for the constant k_1 for Areas 1, 2 and 3 was calculated to the range between 0.00026 and 0.00029, with a standard deviation between 0.000006 and 0.000009 in Table 4.2. This indicates a high consistency across the different Areas, as the variation in the k_1 constant is relatively low. In comparison, the k_1 values used by Ellevio range from 0.00023 to 0.00033, depending on the residential customer subtypes. These results suggest that the calculated global mean value is aligned with the Velander constants used in grid planning.

The global mean value for the constant k_2 for Areas 1 and 2 was calculated to the range 0.0418 and 0.0420, while in Area 3, it was significantly lower at 0.0088, as shown in Table 4.2. While the results in Areas 1 and 2 were closely aligned, Area 3 showed a clear deviation, indicating a fundamental difference in load behaviour. The standard deviation of k_2 ranged from 0.0054 to 0.0078 across all Areas. Although the absolute variation was relatively small, percentage-wise variations in Area 3 were due to its lower global mean value. For comparison, Ellevio uses k_2 values between 0.025 and 0.063, depending on the residential customer subtype. These values align well with Areas 1 and 2 but not in Area 3. In Area 3, the calculated global mean and standard deviation of k_2 were 0.0088 and 0.0065. This proximity suggests high variability relative to the global mean value and supports that the use of Velander constants, at least from this analysis, is not suitable for accurately capturing peak demand in Area 3.

Area 1 and 2 showed similar results in both the mean and standard deviation of the estimated constants k_1 and k_2, while Area 3 showed a significant deviation in the constant k_2. One possible explanation is the difference in the average number of residential customers per substation: Areas 1 and 2 have between 39 and 43 residential customers per substation, while Area 3 has an average of 125. This indicates a higher residential customer density in Area 3, which statistically tends to produce a more evenly distributed and stable load profile. In comparison, the substations in Areas 1 and 2 are more sensitive to variations in individual customer behaviour. As a result, the relationship between peak demand and yearly energy consumption in Area 3 tends to follow a single-variable linear path, where the contribution from the non-linear square root term is reduced. This explains the lower value of k_2, which contributes to the non-linear component in Velander's formula, in Equation 3.11.

4.2 Comparison between REGAL and actual grid

Different types of comparisons were done when comparing the REGAL model with the actual grid, with and without the integration of EVs in both systems.

4.2.1 Capacity comparison

The capacity comparison includes both the aggregated capacity from Ellevio's grid data and the estimated capacity from the REGAL models for selected areas, evaluated with and without EV integration. The aggregated capacity from Ellevio represents the total and residential share from each substation (see Appendix A.6) to A.10 for full substation capacity data), while the estimates from REGAL are based on selected grid cell. The results are based on the Equation 3.16 to 3.19 and are presented in Table 4.3.

Table 4.3: Comparison of REGAL's estimated capacity and Ellevio's residential capacity for all Areas, with and without EVs

Area	EV	$S_{tot}^{Ellevio}$ [kVA]	$S_{res}^{Ellevio}$ [kVA]	$S_{res}^{Ellevio}$ [kVA]	$MAPE$ [%]
1	No	28000	18900	17500	7.5
	Yes		20400		14.2
2	No	45300	24600	30700	25.1
	Yes		27900		10.0
3	No	78800	40550	49700	22.5
	Yes		46000		8.0

The parameter $S_{tot}^{Ellevio}$ refers to the aggregated installed capacity from Ellevio's substations, representing the total available transformer capacity, and the values $S_{res}^{Ellevio}$ correspond to the downscaled portion of this capacity assigned to residential customers. In parallel S_{res}^{REGAL} is the aggregated residential capacity estimated by the REGAL model. The parameter $MAPE$ is used to quantify the percentage deviation between $S_{res}^{Ellevio}$ and S_{res}^{REGAL}.

The capacity comparison table in 4.3 demonstrates that the REGAL model provides a reasonable estimation of the total substation capacity across all Areas. Before the integration of EVs, the deviation ranged from 7.5 to 25.1%, with the lowest deviation in Area 1 and highest in Area 2. These values indicate that REGAL captures the overall dimensions of substations well for the selected Areas.

With the integration of EV charging, the deviations decreased significantly to 10 and 8% in Areas 2 and 3, indicating that the residential capacity is better aligned with the actual scaled residential capacity. However, in Area 1 the deviation increased to 14.2%. This suggests that the deviation can be improved, with the downscaled residential capacity, particularly when the REGAL model overestimates the base load from residential customers.

Overall, the deviation before and after the integration of EVs remains within an acceptable for all three areas with a size between 6 to 8 km^2, particularly in contrast to a higher deviation of 44.5% when comparing individual cells in the REGAL model [6]. However, the REGAL model tends to overestimate the residential capacities in Areas 2 and 3.

4.2.2 Load comparison

This section presents a comparison between the aggregated peak loads from Ellevio's grid data and the REGAL model estimates for the selected areas, both with and without EVs. The aggregated loads from Ellevio correspond to each substation, where the estimates from REGAL are based on selected grid cells. The analysis includes both residential and total load comparisons, where the total load includes commercial loads. The results are based on Equation 3.20 to 3.22 and are presented in Table 4.4.

Table 4.4: Comparison of residential and total loads under different scenarios

Area	EV	**Residential Load**			**Total Load**		
		$P^{max}_{Ellevio}$ [kW]	P^{max}_{REGAL} [kW]	$MAPE$ [%]	$P^{max}_{Ellevio}$ [kW]	P^{max}_{REGAL} [kW]	$MAPE$ [%]
1	No	7900	7500	5	10900	7500	31.2
	Yes	10600	10800	1.9	13200	10800	18.2
2	No	11700	13300	22.2	18200	13300	21.4
	Yes	17200	18500	7.6	22800	18500	18.9
3	No	22000	22200	0.9	37100	22200	40.1
	Yes	29800	34500	15.8	43200	34500	20.1

The parameter $P^{max}_{Ellevio}$ represents the aggregated peak load from Ellevio's substations. In comparison, P^{max}_{REGAL} denotes the aggregated peak load estimated using the REGAL model. The parameter $MAPE$ is used to quantify the percentage deviation between $P^{max}_{Ellevio}$ and P^{max}_{REGAL}.

The results show varying levels of deviation in residential peak load estimation across the three areas. In Area 1, the deviation remained relatively low, decreasing from 5 to 1.9% with EVs. In Area 2, the deviation decreased significantly from 22.2 to 7.6%, with a relatively high deviation without EVs. In contrast, Area 3 showed an opposite trend, the deviation increased from 0.9 to 15.8%, with a relatively high deviation with EVs.

These results indicate that the model's accuracy in estimating residential peak loads is not consistent in all areas, where the inclusion of EVs either improved or worsened its accuracy.

When evaluating the total load, which includes both residential and commercial customers, the deviation was significantly higher. This reduction is expected, as the REGAL model is developed for residential loads and does not include commercial activity in its design. Consequently, this comparison is not entirely representative of REGAL's intended application. The deviation across all areas ranged from 18.9 to 40.1%, which is in general a poorer performance.

It is important to note that the selected areas consist predominantly of residential customers, between 86 to 90% of the total customer base. However, despite the high share, the residential load accounted for only 52 to 70% of the total annual energy consumption. This indicates that even a relatively small portion of commercial customers can have a significant impact on overall energy use. Their presence influences the REGAL model's performance, highlighting its sensitivity to mixed loads and its reduced accuracy when including commercial loads.

In conclusion, the REGAL model demonstrates strong performance in estimating residential peak loads. The overestimations observed in Areas 2 and 3 may arise from local demographic factors not fully captured by the model. While REGAL is not designed for areas with mixed customer compositions, the results highlight both its strengths and limitations. Overall, it is best suited for residential peak load forecasting.

5
Discussion

5.1 Method

The selection criteria for the different areas were specifically designed to align with the structure of the REGAL model, which is designed for only residential customers. Focusing on areas with a high share of residential customers and minimising commercial load influence, which better aligns with REGAL. It also ensures a better comparison between measured data and synthetic estimations, which automatically gives a more reliable evaluation of REGAL's accuracy in a typical residential environment. In addition to the customer share, considering the percentage of residential annual energy consumption would further strengthen the selection process, as it more accurately reflects the actual contribution of residential demand.

However, these selection criteria also limited the ability to draw a general conclusion. By excluding smaller areas, rural areas, and grids with a mixed customer base, where demand is less predictable and individual load behaviour has a greater impact. The analysis focused on where REGAL is expected to perform well. As a result, while REGAL appeared useful in residential-dominated areas with relatively controlled conditions, caution is important when applying it to more complex parts of the grid. Since this study analyses only three areas, further validation is needed using a broader and more diverse set of areas, both similar and different from the selected areas, to more accurately evaluate the general applicability of the REGAL model.

EV charging behaviour was modelled using 170 profiles based on real charging data from actual EV users. These profiles captured realistic variations in charging behaviour, providing a solid foundation for estimating EV demand. In most cases, the number of available EV profiles exceeded the number of EVs per substation, allowing each EV to be assigned a unique EV profile. However, in substations with a high number of EVs, some profiles were reused potentially limiting its diversity. In contrast, substations with only a few EVs, and individual profiles had a large impact. This variation is illustrated in A.11, which shows the average and standard deviation across the 170 profiles.

Lastly, a methodological consideration arises regarding the rescaling of the total substation capacity to isolate the residential capacity. The formulas used in Equation 3.16 and 3.17 assume that the residential peak load directly corresponds to its share of the total capacity. This may oversimplify the actual load behaviour, especially in substations with a large share of commercial customers. Further investigations are needed to determine whether the approach holds under different load compositions.

5.2 Results

The analysis of Velander constants shows similarities in Areas 1 and 2. This is likely due to the estimated number of EVs per residential customer, ranging between 1.1 and 1.24, and the similar average number of residential customers per substation (39-43). In contrast, Area 3 had a higher population density, a lower EV-to-customer ratio of 0.66, and a larger average number of customers per substation, approximately 120. These findings address the Research Question regarding EV-driven loading by suggesting that high EV ownership aligns more closely with Velander constants used by Ellevio (related to research question 3).

Further insights were gained from the analysis of relative load changes in maximum load due to EV integration. Histograms showed that most substations experienced load increases between 0 to 40%, with noticeable variation. Substations with a lower annual energy consumption per customer, typically between 2000 and 8000 kWh were more sensitive to EV integration. In such cases, each additional EV introduced a larger increase in peak demand, amplifying load volatility. This was particularly noticeable in Area 3, where outliers in load increase appeared despite a lower EV per customer ratio of 0.66. While a lower ratio would typically be expected to result in smaller peak load changes, the higher number of residential customers per substation in Area 3 acted as a compensating factor, resulting in peak load changes comparable to those in Areas 1 and 2. These findings reflect both the second and third research questions, demonstrating how REGAL's assumption on EV ownership can still yield comparable peak loads in areas with higher residential density, even when EV ownership is lower.

REGAL's tendency to overestimate peak loads was observed when comparing peak load before and after EV integration was added to the residential load. This overestimating likely arises from the model's design. Each transformer is exposed to multiple iterations of EV charging profiles, with the iteration with the highest peak selected. This effectively models a worst-case scenario without considering its probability. While this approach leads to higher deviations compared to measured data, it can be justified in a grid planning context where conservative estimates ensure a safe margin. For consistency, the same method was when combining Ellevio's residential load profiles with EV charging data, ensuring that both the REGAL and measured datasets reflect extreme case scenarios. These findings address the second research question, highlighting how the structure of REGAL

influences its accuracy in predicting peak load across various assumptions.

When commercial loads are included, the deviation between REGAL estimates and actual peak loads increases, as presented in Table 4.4. Rather than improving estimation accuracy, this highlighted a key limitation of the model, applying the model to a mixed customer base can lead to misleading conclusions. To ensure valid comparisons and reliable results, input use data should reflect primarily only residential loads. This directly addresses the first and second research questions, indicating that REGAL is best suited for grids with predominated residential customer compositions. To improve REGAL's framework, including commercial activity, to provide a broader and more reliable model for its applicability.

Finally, the comparison of capacity and peak loads supports the REGAL applicability in early-stage grid planning within residential areas. The model provides a quick estimation of hosting capacity and peak loads without requiring real-time measurement data. However, in mixed load areas, the accuracy of these estimates was reduced. These observations are related to the first and second research questions, highlighting how assumptions around EV behaviour and customer types influence transformation utilization or potential overloading.
In areas where REGAL's assumptions closely match actual conditions, the model performs well. However, when assumptions such as car ownership or customer composition deviate from reality, REGAL may over or underestimate future demand. This underscores the importance of aligning model assumptions with local conditions for accurate grid planning.

5.3 Future work

Future work could expand by using power flow simulations in the low voltage grid to analyse how EV charging affects the voltage profile, line loading and system losses. This would require implementing a power flow method such as Newton-Raphson or backward/forward sweep algorithm to capture the grid behaviour under varying loads.

Another future work involves the investigation of V2G integration in a radial low-voltage grid. Since V2G introduced bidirectional power flows, where it challenges the current top-down voltage drops in radial systems. This raises an important question about voltage regulations and protection schemes when current flows are in reverse directions, which is critical for future grid systems.

Finally, further validation of the REGAL model could involve additional parameter comparisons such as cable lengths, voltage drops and customer-type variability. Specifically testing REGAL in areas with lower population density or higher customer diversity could help to determine the model's robustness, accuracy and grid planning applications.

6
Conclusion

This thesis evaluated the applicability of the REGAL model for grid planning in Ellevio's LV grid under a 100% EV penetration scenario. The study focused on understanding how EV integration affects substation loading and how accurately REGAL estimates peak loads and residential capacities. By using measured load data from multiple customers, EV charging data, and substations level analysis across three areas, the study investigated REGAL's performance under varying residential densities and customer compositions.

The results show that REGAL can be a useful tool for grid planning, particularly in areas with a high share of residential customers and limited commercial customers. REGAL's peak estimation aligned when only considering residential load. However, in areas with mixed customer types or significant commercial loads, it resulted in larger deviations. This indicates that REGAL is most suited for planning in residential-dominated areas, where its core assumptions are more valid.

The accuracy of REGAL's peak load estimates was shown to depend strongly on assumptions such as EV ownership, customer density and load composition. In Area 3, where the EV ownership was lower, the peak loads were comparable with Area 2 and 3 due to the higher number of customers per substation. This highlights that REGAL's assumptions can compensate for each other, but also underscores the importance of aligning the model with local conditions to avoid misleading results.

The impact of high EV penetration on the LV loading was observed, Most substations experienced increases up to 40%, but REGAL tended to overestimate these peaks due to its usage of worst-case scenario selections. While this conservative approach ensures safety margins, it may lead to unnecessary high infrastructure investments if used without additional context. Still, worst-case estimates can be valuable in long-term grid planning.

In summary, REGAL demonstrates a strong potential for grid planning in residential areas. However, to strengthen and generalize the model's applicability, further analysis across a wider range of areas is needed. Including commercial loads and performing more parameter comparisons, would provide a more complete evaluation of the model's performance. With these improvements, REGAL could play a central role in building robust and future-proof LV grids.

Bibliography

[1] T. Nogueira, E. Sousa, and G. R. Alves, "Electric vehicles growth until 2030: Impact on the distribution network power," *Energy Reports*, vol. 8, pp. 145–152, 2022, The 8th International Conference on Energy and Environment Research –"Developing the World in 2021 with Clean and Safe Energy", ISSN: 2352-4847. DOI: https://doi.org/10.1016/j.egyr.2022.01.106. [Online]. Available: https://www.sciencedirect.com/science/article/pii/S2352484722001068.

[2] "Zero emission vehicles first fit for 55 deal will end the sale of new co2 emitting cars in europe by 2035," Oct. 2022. [Online]. Available: https://ec.europa.eu/commission/presscorner/api/files/document/print/en/ip_22_6462/IP_22_6462_EN.pdf.

[3] P. Circle. "Power circle summerar elbilsåret 2024." (2024), [Online]. Available: https://press.powercircle.org/posts/pressreleases/power-circle-summerar-elbilsaret-2024 (visited on 02/05/2025).

[4] ACEA. "Report: Vehicles on european roads 2025." (2025), [Online]. Available: https://www.acea.auto/publication/report-vehicles-on-european-roads-2025/ (visited on 02/05/2025).

[5] J. Sarda *et al.*, *A review of the electric vehicle charging technology, impact on grid integration, policy consequences, challenges and future trends*, Dec. 2024. DOI: 10.1016/j.egyr.2024.11.047.

[6] T. Lundblad, M. Taljegard, N. Mattsson, E. Hartvigsson, and F. Johnsson, "An open data-based model for generating a synthetic low-voltage grid to estimate hosting capacity," *Sustainable Energy, Grids and Networks*, vol. 39, p. 101 483, 2024, ISSN: 2352-4677. DOI: https://doi.org/10.1016/j.segan.2024.101483. [Online]. Available: https://www.sciencedirect.com/science/article/pii/S2352467724002121.

[7] Ellevio. "Ellevio now and then." Accessed: 2025-01-21. (2024), [Online]. Available: https://www.ellevio.se/en/about-us/about-the-company/ellevio-now-and-then/#h-facts-about-ellevio.

[8] A. M. P. Barros, J. H. Angelim, and C. M. Affonso, "Impact on distribution transformer life using electric vehicles with long-range battery capacity," *Energies*, vol. 16, no. 12, p. 4810, 2023. DOI: 10.3390/en16124810. [Online]. Available: https://www.mdpi.com/1996-1073/16/12/4810.

[9] A. Jain and M. Karimi-Ghartemani, "Mitigating adverse impacts of increased electric vehicle charging on distribution transformers," *Energies*, vol. 15, no. 23, p. 9023, 2022. DOI: 10.3390/en15239023. [Online]. Available: https://doi.org/10.3390/en15239023.

[10] Ö. Polat, O. H. Eyüboğlu, and Ö. Gül, "Monte carlo simulation of electric vehicle loads with respect to return home from work and impacts on the low voltage side of the distribution network," English, *Electrical Engineering*, vol. 103, no. 1, pp. 439–445, Feb. 2021, ISSN: 0948-7921. DOI: 10.1007/s00202-020-01093-5.

[11] D. Garcia Aguilar *et al.*, *Investigating the impact of electric vehicle charging loads on csun's electric grid*, arXiv preprint arXiv:2409.12876, Accessed: 2025-06-12, Sep. 2024. DOI: 10.48550/arXiv.2409.12876. [Online]. Available: https://arxiv.org/abs/2409.12876.

[12] S. Zaferanlouei, V. Lakshmanan, S. Bjarghov, H. Farahmand, and M. Korpås, "Battpower application: Large-scale integration of evs in an active distribution grid – a norwegian case study," *Electric Power Systems Research*, vol. 210, p. 107 967, 2022. DOI: 10.1016/j.epsr.2022.107967.

[13] T. Kerdphol, "Leveraging vehicle-to-grid technology for sharing synthetic inertia in renewable-dominant grids," *Electric Power Systems Research*, vol. 241, p. 111 405, Apr. 2025. DOI: 10.1016/j.epsr.2024.111405. [Online]. Available: https://doi.org/10.1016/j.epsr.2024.111405.

[14] M. Hungbo, M. Gu, L. Meegahapola, T. Littler, and S. Bu, "Impact of electric vehicles on low-voltage residential distribution networks: A probabilistic analysis," *IET Smart Grid*, vol. 6, no. 5, pp. 536–548, Aug. 2023, Open Access. DOI: 10.1049/stg2.12123. [Online]. Available: https://doi.org/10.1049/stg2.12123.

[15] I. Chandra, N. K. Singh, P. Samuel, M. Bajaj, A. R. Singh, and I. Zaitsev, "Optimal scheduling of solar powered ev charging stations in a radial distribution system using opposition-based competitive swarm optimization," *Scientific Reports*, vol. 15, no. 1, Article 4880, Dec. 2025, ISSN: 2045-2322. DOI: 10.1038/s41598-025-88758-y. [Online]. Available: https://doi.org/10.1038/s41598-025-88758-y.

[16] A. Nordling, "Sveriges framtida elnät," Kungl. Ingenjörsvetenskapsakademien (IVA), IVA-M 464, 2024. [Online]. Available: https://www.iva.se/contentassets/8cd3b42561e34e11813dc96eee192132/ivavagvalel-sveriges-framtida-elnat.pdf (visited on 02/07/2025).

[17] Energimarknadsinspektionen, *Nätkoncession – tillstånd att bygga och använda en elledning*, Accessed: 2025-06-11, Energimarknadsinspektionen, 2022. [Online]. Available: https://www.ei.se/konsument/el/elnat/natkoncession.

[18] Energimarknadsinspektionen. "Ansökan om nätkoncession för område." Accessed: 2025-06-11, Swedish Energy Markets Inspectorate. (2023), [Online]. Available: https://ei.se/bransch/koncessioner/ansokan-om-natkoncession-for-omrade.

[19] E. Technology. "Uses and applications of transformer." Accessed: 2025-02-11. (2012), [Online]. Available: https://www.electricaltechnology.org/2012/02/uses-and-application-of-transformer.html.

[20] S. Basics. "The key components of an electrical substation." Accessed: 2025-02-11. (2023), [Online]. Available: https://substationbasics.com/the-key-components-of-an-electrical-substation/.

[21] W. Hardware. "What are electrical busbars? types, advantages, and applications." Accessed: 2025-02-11. (2024), [Online]. Available: https://www.worthyhardware.com/news/what-are-electrical-busbars-types-advantages-and-applications/.

[22] Vattenfall Eldistribution AB. "Teknikval." Accessed: 2025-06-11, Vattenfall Eldistribution AB. (n.d.), [Online]. Available: https://www.vattenfalleldistribution.se/var-verksamhet/om-elnatet/elnatets-uppbyggnad/teknikval/.

[23] R. Hurst. "Transmission lines: Types, function & grid infrastructure." Accessed: 2025-02-11. (2023), [Online]. Available: https://electricityforum.com/td/overhead-td/transmission-lines.

[24] Vattenfall Eldistribution AB. "Luftledning." Accessed: 2025-06-11, Vattenfall Eldistribution AB. (n.d.), [Online]. Available: https://www.vattenfalleldistribution.se/var-verksamhet/om-elnatet/elnatets-uppbyggnad/teknikval/luftledning/.

[25] Vattenfall Eldistribution AB. "Markkabel." Accessed: 2025-06-11, Vattenfall Eldistribution AB. (n.d.), [Online]. Available: https://www.vattenfalleldistribution.se/var-verksamhet/om-elnatet/elnatets-uppbyggnad/teknikval/markkabel/.

[26] Vattenfall Eldistribution AB. "Sjökabel." Accessed: 2025-06-11, Vattenfall Eldistribution AB. (n.d.), [Online]. Available: https://www.vattenfalleldistribution.se/var-verksamhet/om-elnatet/elnatets-uppbyggnad/teknikval/sjokabel/.

[27] A. D. Rodriguez, F. Martinez Fuentes, and A. Jaramillo Matta, "Analysis of renewable energy integration in the colombian power system," in *2015 Workshop on Engineering Applications (WEA)*, Bogotá, Colombia: IEEE, Oct. 2015, pp. 1–6, ISBN: 978-1-5090-0228-3. DOI: 10.1109/WEA.2015.7370122. [Online]. Available: https://ieeexplore.ieee.org/document/7370122.

[28] H. Markiewicz and A. Klajn, "En 50160: Voltage characteristics of electricity supplied by public distribution systems," Wroclaw University of Technology, Tech. Rep., Jul. 2004. [Online]. Available: https://www.evm.ua/image/catalog/uslugi/standart-en-50160.pdf.

[29] A. Boricic, J. L. R. Torres, and M. Popov, "System strength: Classification, evaluation methods, and emerging challenges in ibr-dominated grids," in *Proceedings of the 11th International Conference on Innovative Smart Grid Technologies - Asia, ISGT-Asia 2022*, IEEE, 2022, pp. 185–189. DOI: 10.1109/ISGTAsia54193.2022.10003499. [Online]. Available: https://doi.org/10.1109/ISGTAsia54193.2022.10003499.

[30] M. Sandström, C. Bales, and E. Dotzauer, "Hosting Capacity of the Power Grid for Electric Vehicles - A Case Study on a Swedish Low Voltage Grid," vol. 1050, no. 1, 2022, ISSN: 17551315. DOI: 10.1088/1755-1315/1050/1/012008.

[31] SSS Clutch Company, Inc., *Short-circuit level and electricity system strength*, Accessed: 2025-02-17, 2024. [Online]. Available: https://www.sssclutch.com/en/articles/short-circuit-level-and-electricity-system-strength/.

[32] A. Yadav, N. Kishor, and R. Negi, "Voltage profile analysis in distribution network for allowable hosting capacity from pv integration," in *2022 1st International Conference on Sustainable Technology for Power and Energy Systems (STPES)*, 2022, pp. 1–6. DOI: 10.1109/STPES54845.2022.10006593.

[33] J. Caballero-Peña, G. Osma-Pinto, and C. Cadena-Zarate, "Distributed energy resources on distribution networks: A systematic review of modelling, simulation, metrics, and impacts," *International Journal of Electrical Power & Energy Systems*, vol. 138, p. 107 900, 2022. DOI: 10.1016/j.ijepes.2021.107900. [Online]. Available: https://doi.org/10.1016/j.ijepes.2021.107900.

[34] North American Electric Reliability Corporation. "An introduction to inverter-based resources on the bulk power system." Accessed: 2025-02-13. (Jun. 2023), [Online]. Available: https://www.nerc.com/pa/Documents/2023_NERC_Guide_Inverter-Based-Resources.pdf.

[35] E. Mengelkamp, J. Gärttner, K. Rock, S. Kessler, L. Orsini, and C. Weinhardt, "Designing microgrid energy markets: A case study for a german community," *Applied Energy*, vol. 210, pp. 870–880, 2018. DOI: 10.1016/j.apenergy.2017.06.054. [Online]. Available: https://doi.org/10.1016/j.apenergy.2017.06.054.

[36] J. He, Y. W. Li, and F. Blaabjerg, "An enhanced islanding microgrid reactive power, imbalance power, and harmonic power sharing scheme," *IEEE Transactions on Power Electronics*, vol. 30, no. 6, pp. 3389–3401, 2015. DOI: 10.1109/TPEL.2014.2332998. [Online]. Available: https://doi.org/10.1109/TPEL.2014.2332998.

[37] A. T. Procopiou, K. Petrou, and L. (Ochoa. "Advanced planning of pv-rich distribution networks – deliverable 3: Traditional solutions." Accessed: 2025-02-11. (2020), [Online]. Available: https://doi.org/10.13140/RG.2.2.27813.45286/1.

[38] S. Maharjan, D. S. Kumar, and A. M. Khambadkone, "Enhancing the voltage stability of distribution network during pv ramping conditions with variable speed drive loads," *Applied Energy*, vol. 264, 2020, ISSN: 0306-2619. DOI: 10.1016/j.apenergy.2020.114733. [Online]. Available: https://doi.org/10.1016/j.apenergy.2020.114733.

[39] A. Demazy, T. Alpcan, and I. Mareels, "A probabilistic reverse power flows scenario analysis framework," *IEEE Open Access Journal of Power and Energy*, vol. 7, pp. 524–532, 2020. DOI: 10.1109/OAJPE.2020.3032902.

[40] How Electrical. "Radial distribution system: Definition, advantages, and disadvantages." Accessed: 2025-06-11. (2023), [Online]. Available: https://howelectrical.com/radial-distribution-system/.

[41] A. Charfi, M. Ayadi, H. Ben Hamed, and A. Bouallegue, "Harmonics impact of electric vehicle charging on power quality in distribution systems," in *Proceedings of the International Conference on Energy, Green Hydrogen and Sustainability (ICEGS 2023)*, ser. E3S Web of Conferences, vol. 437, EDP Sciences, 2023, p. 00 054. DOI: 10.1051/e3sconf/202343700054. [Online]. Available: https://www.e3s-conferences.org/articles/e3sconf/pdf/2023/106/e3sconf_icegc2023_00054.pdf.

A

Appendix 1

A.1 Customer distribution

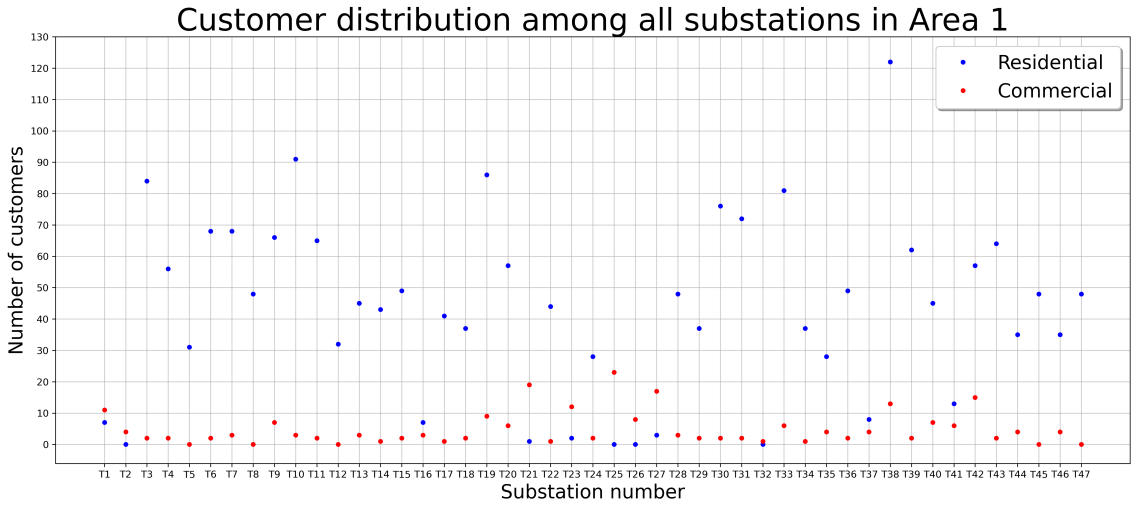

Figure A.1: Area 1: Residential and commercial customer count across all substations

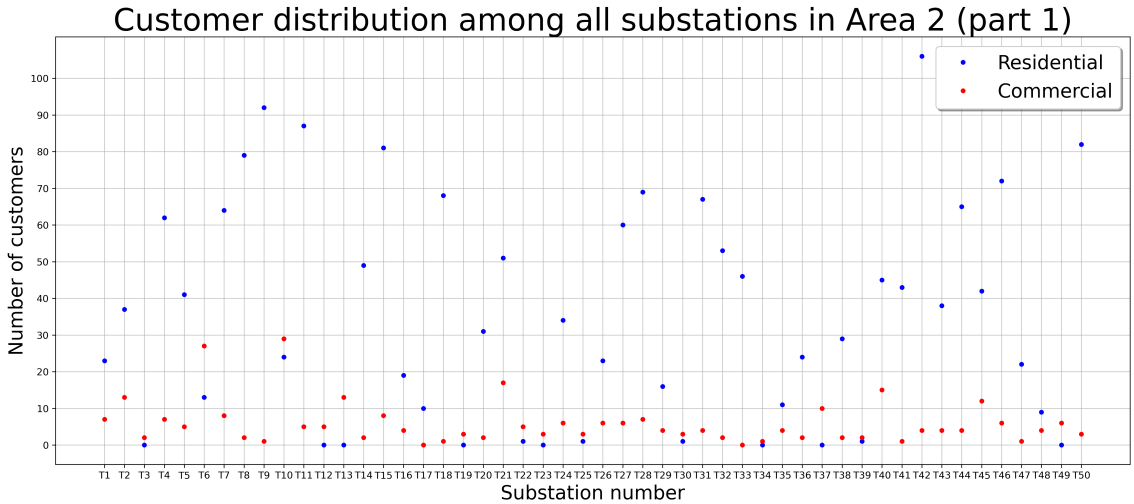

Figure A.2: Area 2: Residential and commercial customer count across all substations (part 1)

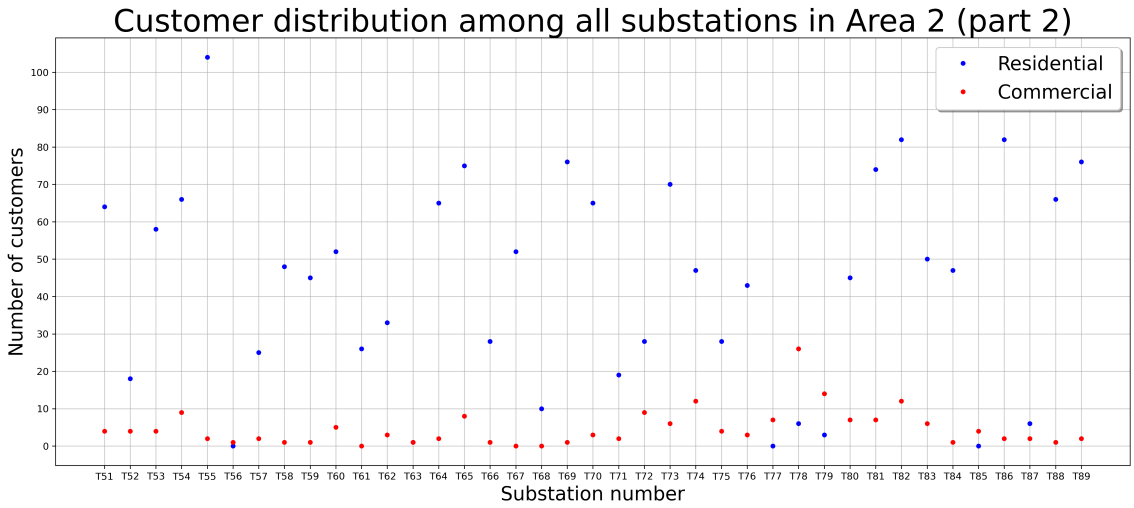

Figure A.3: Area 2: Residential and commercial customer count across all substations (part 2)

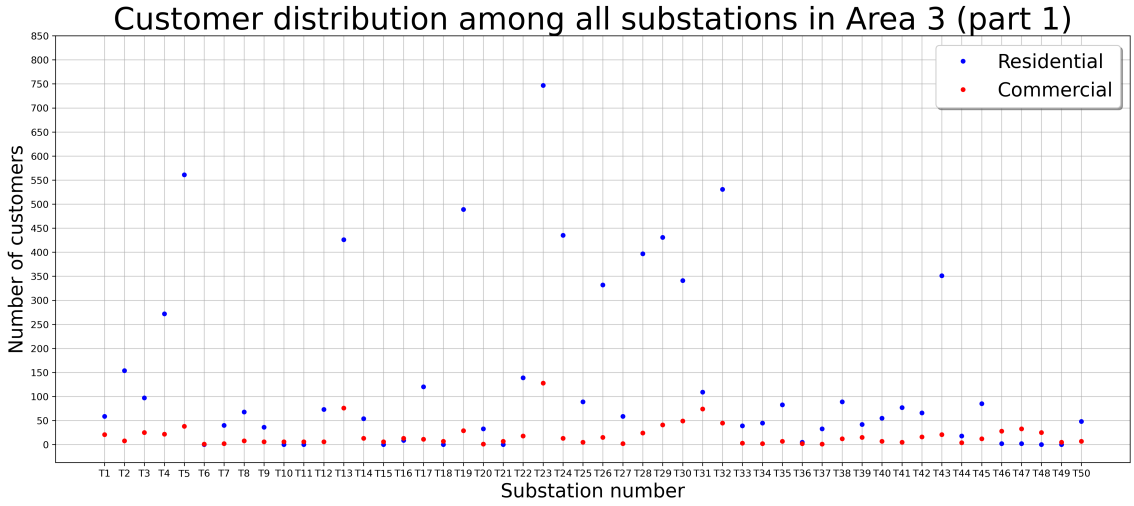

Figure A.4: Area 3: Residential and commercial customer count across all substations (part 1)

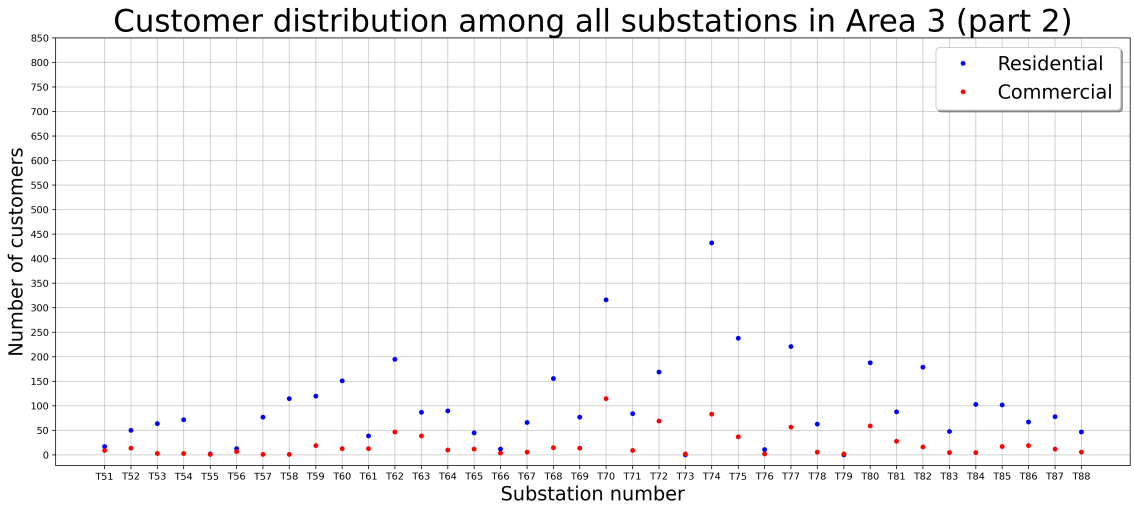

Figure A.5: Area 3: Residential and commercial customer count across all substations (part 2)

A.2 Rated capacity distribution

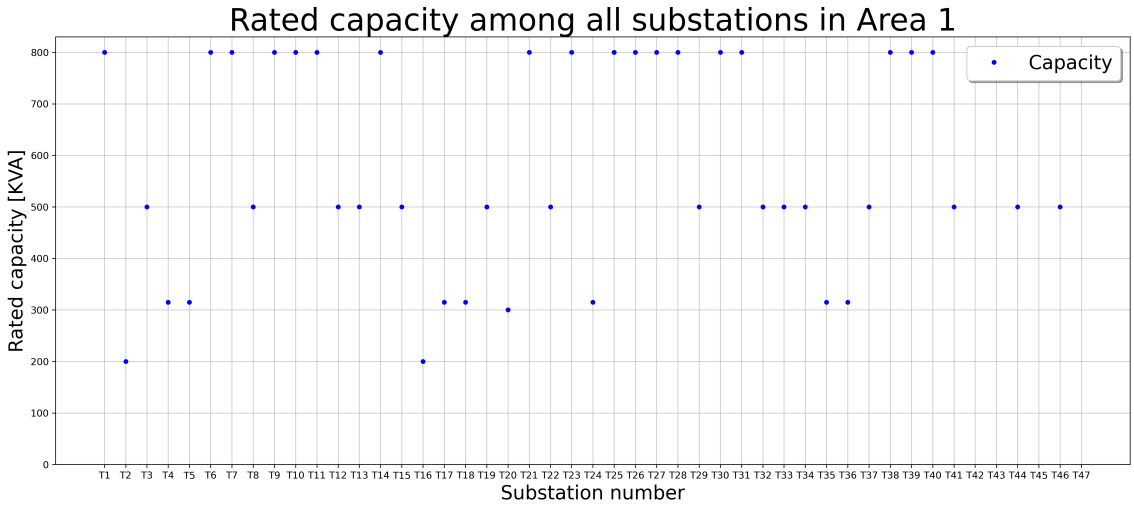

Figure A.6: Area 1: Rated capacity across all substations

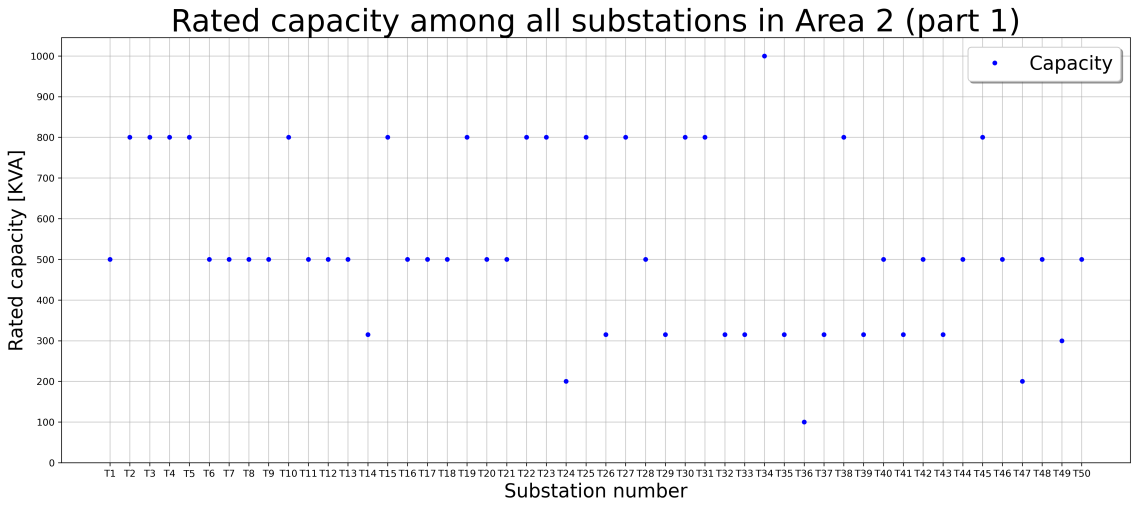

Figure A.7: Area 2: Rated capacity across all substations (part 1)

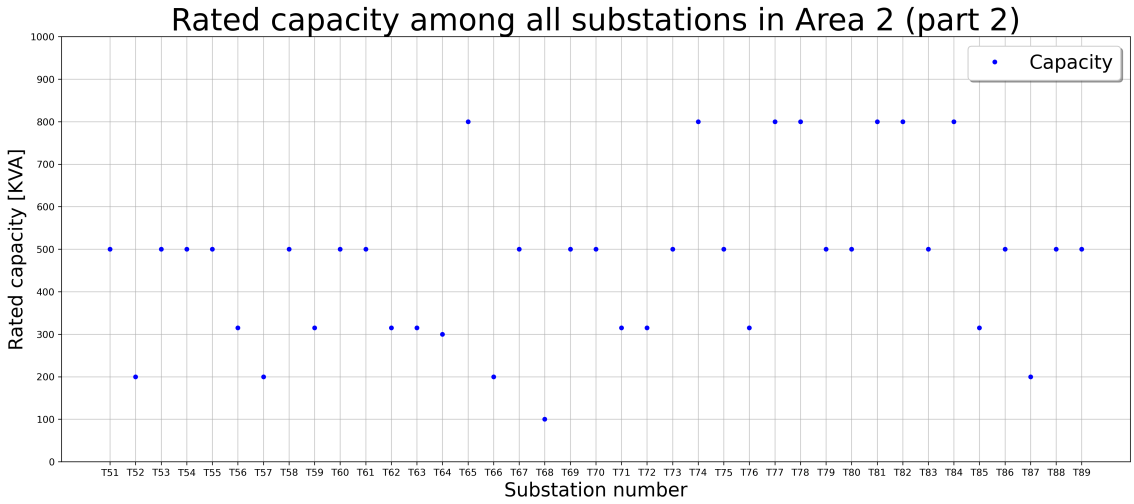

Figure A.8: Area 2: Rated capacity across all substations (part 2)

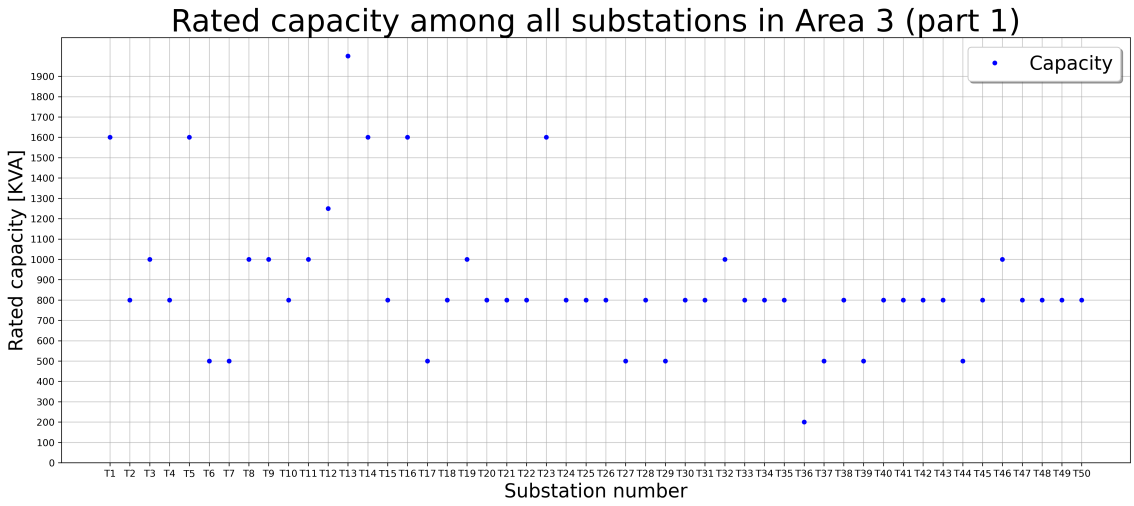

Figure A.9: Area 3: Rated capacity across all substations (part 1)

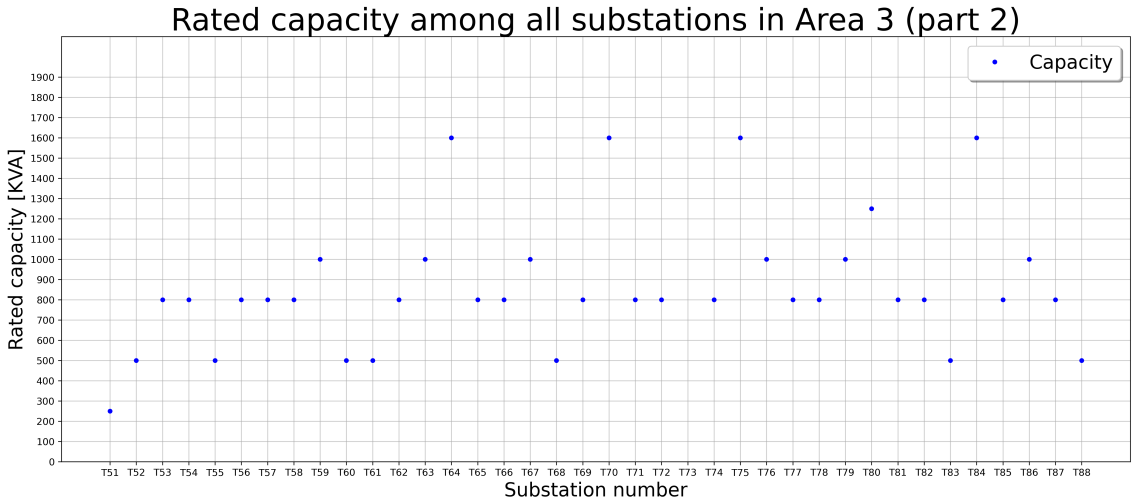

Figure A.10: Area 3: Rated capacity across all substations (part 2)

A.3 Average load profiles

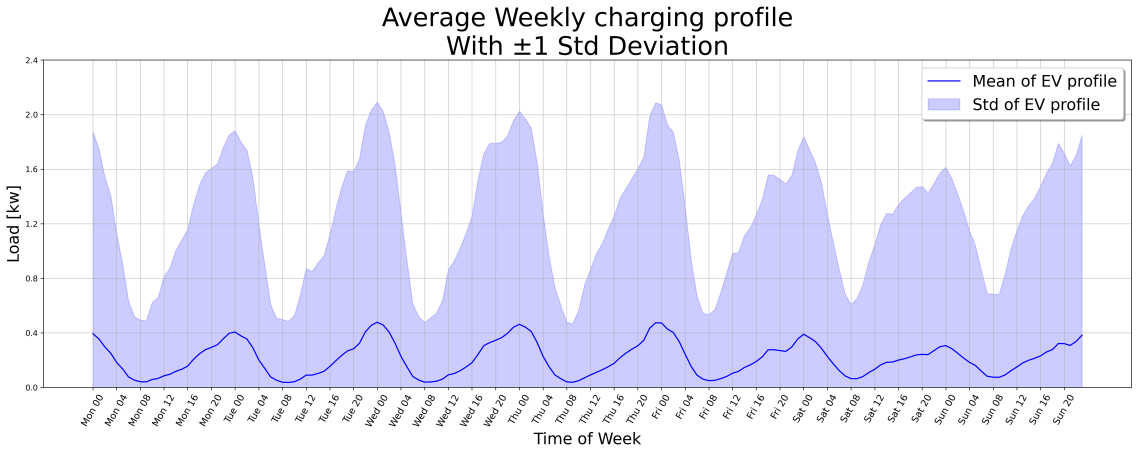

Figure A.11: Average weekly load profile for the 170 EV profiles. With mean and standard deviation

DEPARTMENT OF EARTH SPACE AND ENVIRONMENT
CHALMERS UNIVERSITY OF TECHNOLOGY
Gothenburg, Sweden
www.chalmers.se

CHALMERS
UNIVERSITY OF TECHNOLOGY